Coordination Chemistry Reviews 254 (2010) 197–214

Contents lists available at ScienceDirect

Coordination Chemistry Reviews

journal homepage: www.elsevier.com/locate/ccr

Review

Oxo ligand functionalization in the uranyl ion (UO_2^{2+})

Skye Fortier, Trevor W. Hayton *

Department of Chemistry and Biochemistry, University of California Santa Barbara, Santa Barbara, CA 93106, United States

Contents

ARTICLE INFO

Article history:
Received 12 March 2009
Accepted 12 June 2009
Available online 21 June 2009

Keywords:
Actinyl ions
Uranyl kinetics
Cation–cation interactions
Oxo substitution
Oxo functionalization

ABSTRACT

Uranyl (UO_2^{2+}) is an exceptionally stable molecular species, characterized by a linear O=U=O geometry and short U–O bonds. Its two oxo ligands are thought to be inert to exchange and resistant to functionalization. However, a growing body of literature suggests that this assessment may need to be reevaluated. This review summarizes the chemistry of the two oxo ligands of the uranyl ion. In particular, we explore the interaction of the uranyl oxo ligands with Lewis acids, and outline attempts to selectively functionalize the oxo ligands of uranyl by chemical means. We also discuss the kinetic and mechanistic knowledge for oxo ligand exchange under acidic, basic and photolytic conditions.

1. Introduction

Several reviews have recently appeared which outline the chemistry of the uranyl ion [1–5], including articles that focus on the kinetics and mechanism of equatorial ligand exchange [1], the synthesis and characterization of pentavalent uranyl (UO_2^{+}) [2,3], the bioinorganic chemistry of uranyl [4], and the complexation

* Corresponding author.
E-mail address: hayton@chem.ucsb.edu (T.W. Hayton).

0010-8545/$ – see front matter © 2009 Elsevier B.V. All rights reserved.
doi:10.1016/j.ccr.2009.06.003

of uranyl with N-donor ligands [5]. These above mentioned articles have focused mostly on the coordination of ligands to the uranyl equatorial plane. In contrast, the emphasis of this review will be the reactivity of the two axial oxo ligands of the uranyl moiety, the so-called "yl" oxygens, and the kinetics and mechanism of these transformations. The reactivity of the "yl" oxygens has gained considerable interest in recent years, and thus we feel a review of this topic is both timely and useful. Instances of "yl" oxygen functionalization are appearing in the literature with increasing frequency. However, processes that effect the substitution and/or functionalization of the uranyl oxo ligands are still relatively rare. By understanding how to effect the selective functionalization of uranyl, novel strategies for waste treatment and environmental remediation may be realized. In this regard, we hope this contribution will spur further development in this area.

This review is divided into four main sections: (a) Ligand coordination in the equatorial plane, (b) Interaction of the "yl" oxygen atoms with Lewis acids, (c) Synthetic approaches for U–O bond cleavage, and (d) Kinetics and mechanism of uranyl oxo ligand exchange. Much of this contribution focuses on synthesis and structural characterization; however, we have also reviewed the relevant kinetic and mechanistic literature pertaining to oxo ligand exchange.

2. Ligand coordination in the uranyl equatorial plane

The uranyl (UO_2^{2+}) fragment is uniquely characterized by short U–O(oxo) bond lengths (ca. 1.78 Å) and a linear O–U–O geometry [6], and it rarely deviates from these parameters. Perturbations of the O–U–O angle are usually small (ca. 5°) [7], and rarely exceed 10°, such as in $[Cp^*UO_2(CN)_3]^{2-}$ (168.40(9)°) and $UO_2(OAr)_2(thf)_2$ (Ar = 2,6-^{t}Bu$_2$C$_6$H$_3$) (167.8(4)°) [8,9], however these instances are uncommon. Uranyl co-ligands are almost always confined within the equatorial plane that lies perpendicular to the O–U–O vector. Deviations out of the plane are rare and usually require bulky, chelating ligands to be observed. It has also been suggested that out-of-plane coordination is more likely with N donors [10]. For example, out-of-plane coordination is found in $[UO_2(phen)_3]^{2+}$, where the N atoms of the 1,10-phenanthroline ligand are displaced out of the equatorial plane by an average of 0.60 Å [11,12]. In fact, the coordination geometry of this complex is better described as a bicapped octahedron than the expected hexagonal bipyramid. In another example, the N atoms in $[UO_2(NCN)_3]^-$ (NCN^- = $[PhC(NSiMe_3)_2]^-$) are displaced out of the equatorial plane by an average of 0.51 Å [10].

The geometry of the uranyl fragment is also maintained when it is reduced to its pentavalent state (e.g., UO_2^+). Structural studies of $[UO_2(py)_5][KI_2(Py)_2]$ [13,14], $[UO_2(OPPh_3)_4][OTf]$ [15], and $\{[UO_2(dbm)_2]_4[K_6(Py)_{10}]\}^{2+}$ [16], reveal slightly longer U–O_{yl} bond lengths than those observed for UO_2^{2+} [6,17]. However, the O–U–O angles are still linear, revealing the underlying uranyl character of this ion. Examples of out-of-plane coordination for the equatorial ligands in UO_2^+ have yet to be observed, but this may simply be a consequence of the limited number of samples that have been structurally characterized.

In 1 M $HClO_4$ uranyl is coordinated by five waters of solvation (e.g., $[UO_2(H_2O)_5]^{2+}$) [18]. This structure is also observed for the perchlorate salt in the solid-state [19]. The formal reduction potential for UO_2^{2+}(aq) has been measured numerous times, and the accepted literature value is 0.062 V (vs. NHE) [20–22]. A more recent measurement using cyclic voltammetry places the reduction potential at −0.169 V (vs. Ag/AgCl) [23]. A selection of U(VI)/U(V) reduction potentials for a number of uranium(VI) complexes, including UO_2^{2+}(aq), is shown in Fig. 1. The observed values span a large range, from 1.91 V for UF_6 to −1.12 V for U(O^tBu)$_6$ (all values vs. Fc/Fc^+) [24,25]. These redox potentials can be grouped into two clusters. The first group consists of strong oxidants, namely UF_6 and UCl_6. These two complexes contain simple anionic ligands and exhibit a predominantly ionic metal–ligand bonding interaction. The reduction potential of UCl_6 has not been measured directly, however a cyclic voltammogram of $[NBu_3Me]_2[UCl_6]$ in $[NBu_3Me][Tf_2N]$ reveals a U(IV)/U(V) couple at 0.01 V (vs. Fc/Fc^+) but is devoid of any other oxidation feature out to a potential of 0.8 V (vs. Fc/Fc^+), allowing us to estimate a lower limit for the U(V)/U(VI) oxidation potential [26,27].

The second group of complexes lies at the other end of the potential range. These complexes are poor oxidants. Additionally, they are characterized by strongly π-donating ligands and the presence of reasonably covalent metal–ligand bonding interactions. Not surprisingly, uranyl exhibits a potential in-line with its strongly π-donating oxo ligands, comparable to the other U(VI) complexes which also contain strong π-donors.

The reduction potentials for many uranyl complexes are also known and a selection of these values is shown in Fig. 2. The ligands coordinated to the uranyl equatorial plane have a profound effect on the observed U(VI)/U(V) redox potentials. The largest reduction potentials belong to neutral complexes containing strongly electron donating ligands, such as diketiminates and diketonates (Fig. 2) [31,32]. As a result, powerful reducing agents, such as Cp_2^*Co, are required to effect their one-electron reduction [31]. Weaker donors, such as acetate and DMSO, tend to have a smaller affect on the UO_2^{2+} reduction potential [23,33].

The coordination of strongly donating ligands to uranyl is also reflected in the symmetric U=O stretch (ν_1) and the asymmetric U=O stretch (ν_3). For instance, in $[UO_2(H_2O)_5]^{2+}$, ν_3 is 962 cm^{-1} while ν_1 is 870 cm^{-1} [34,35]. Upon coordination of strong electron-

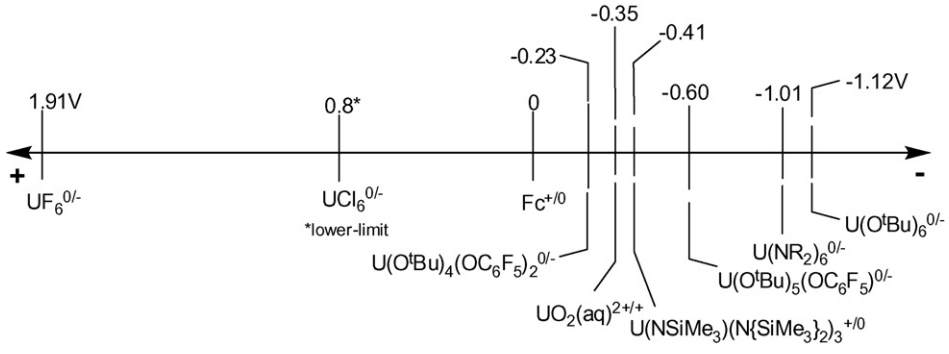

Fig. 1. U(VI)/U(V) reduction potentials (vs. Fc/Fc^+) for selected U(VI) complexes. Reduction potential for UF_6 taken from Ref. [24]. Oxidation potential for U($NSiMe_3$)($N\{SiMe_3\}_2$)$_3$ taken from Ref. [28]. Reduction potential for U(O^tBu)$_6$ taken from Ref. [25]. Reduction potentials for U(O^tBu)$_{6-n}$(OC_6F_5)$_n$ (n = 1, 2) taken from Ref. [29]. Oxidation potentials for U(NR_2)$_6^-$ (HNR_2 = 2,3:5,6-dibenzo-7-azabicyclo[2.2.1]hepta-2,5-diene) taken from Ref. [30]. Reduction potential for $[UO_2(H_2O)_5]^{2+}$ taken from Ref. [23].

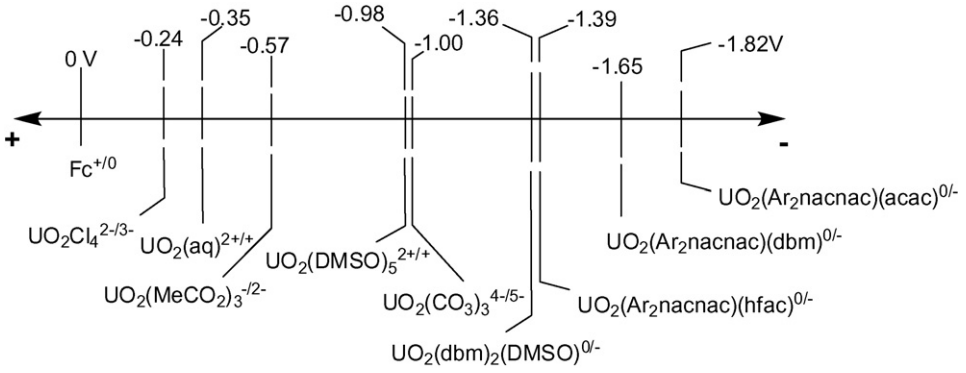

Fig. 2. U(VI)/U(V) reduction potentials (vs. Fc/Fc^+) of selected uranyl complexes. Reduction potentials for $[UO_2(MeCO_2)_3]^{2-}$, $[UO_2(H_2O)_5]^{2+}$, $[UO_2Cl_4]^{2-}$ and $[UO_2(CO_3)_3]^{4-}$ taken from Ref. [23]. Reduction potentials for UO_2(Ar2nacnac)(acac), UO_2(Ar2nacnac)(dbm), UO_2(Ar2nacnac)(hfac) taken from Ref. [31]. Reduction potential for $UO_2(dbm)_2(DMSO)$ taken from Ref. [32]. Reduction potential for $[UO_2(DMSO)_5]^{2+}$ taken from Ref. [33]. Ar2nacnac = [(2,6-^{i}Pr$_2$C$_6$H$_3$)*N*C(Me)CHC(Me)*N*(2,6-^{i}Pr$_2$C$_6$H$_3$)]$^-$; dbm = [PhC(*O*)CHC(*O*)Ph]$^-$; hfac = [CF_3C(*O*)CHC(*O*)CF_3]$^-$.

donating ligands these values drop by ca. 30–60 cm^{-1} [35,36]. For example, in $[UO_2(C_2O_4)_3]^{4-}$ ν_1 is observed at 825 cm^{-1} [35]. Likewise, in *trans*-$UO_2(thf)_2(OAr)_2$ (Ar = 2,6-$Ph_2C_6H_3$) ν_1 is observed at 808 cm^{-1} [9]. This change in U=O stretching frequency is usually attributed to a weakening of the U=O bond upon complexation of a strong donor [10,34–37]. Sarsfield and coworkers have used the U=O symmetric stretch as a guide for predicting oxo ligand reactivity [38], and this concept will be explored in detail in the next section. Moreover, a reasonable correlation exists between ν_1 and the uranyl(VI)/(V) redox potential for several complexes, including $[UO_2(O_2CMe)_3]^-$, UO_2^{2+}(aq), $[UO_2(OH)_4]^{2-}$, and $[UO_2(CO_3)_3]^{4-}$ (Fig. 3) [23,35,39]. Interestingly, $[UO_2Cl_4]^{2-}$ does not fit this trend, as it is unexpectedly easier to reduce than UO_2^{2+}(aq) [23]. In contrast to the Raman spectroscopy results, our survey of the literature found no correlation between reduction potential and ν_3, possibly because of the difficulty in accurately assigning this vibrational mode, as it often overlaps with ligand vibrations [40].

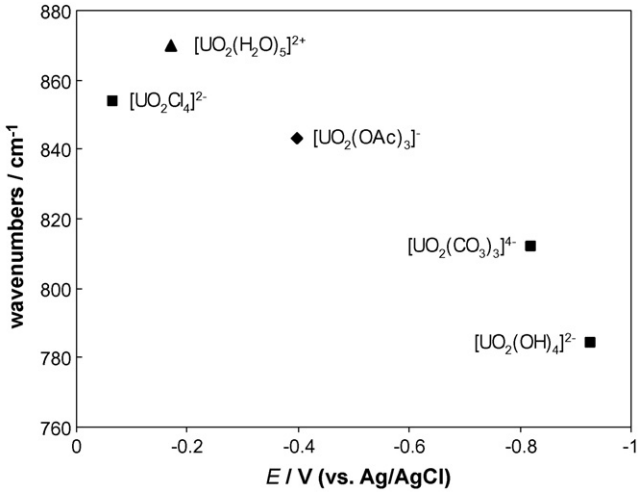

Fig. 3. Comparison of symmetric U=O vibration (ν_1) and the uranyl(VI) reduction potential for a selection of uranyl complexes (vs. Ag/AgCl). Reduction potentials taken from Ref. [23]. Raman data for $[UO_2(O_2CMe)_3]^-$, UO_2^{2+}(aq), $[UO_2Cl_4]^{2-}$, and $[UO_2(CO_3)_3]^{4-}$ taken from Ref. [35]. Raman data for $[UO_2(OH)_4]^{2-}$ taken from Ref. [39].

The electron donating ability of the equatorial ligand set plays an important role in activating the oxo ligands towards functionalization and/or substitution. By increasing the electron density at the uranium metal center, it has been argued that the electrostatic repulsion between the metal and "yl" oxygen atoms is increased, thereby increasing their Lewis basicity [36,41,42]. While the nature of equatorial ligand bonding is still being debated, Clark and coworkers have postulated that π-donating ligands can compete for the 6d orbitals involved in the U–O_{yl} π-bond, making strong π-donor ligands better 'activators' of the U=O bond [39]. However, a subsequent DFT analysis on $[UO_2(H_2O)_m(OH)_n]^{2-n}$ ($n+m=5$) by Kaltsoyannis and coworkers provided no evidence for competition of the 6d atomic orbitals between U–O_{yl} and U–OH [42].

3. Interaction of the "yl" oxygen atoms with Lewis acids

This section explores the interactions of the "yl" oxygen atoms with Lewis acids, both in discrete molecules and in extended solids. We also summarize the literature pertaining to uranyl cation–cation interactions (CCI's), an important subclass of uranyl–Lewis acid complexes that is relevant to both nuclear fuel processing and the kinetics and mechanism of oxo ligand exchange.

3.1. Uranyl–cation interactions in discrete molecules

Uranyl–cation interactions in discrete molecules are relatively rare, but they can be promoted by tuning the equatorial ligand environment of the uranyl moiety. Addition of strong σ-donating ligands, such as hydroxides [39], alkoxides [43], and amides [10,44], have been shown to weaken the U–O_{yl} bond. This phenomenon

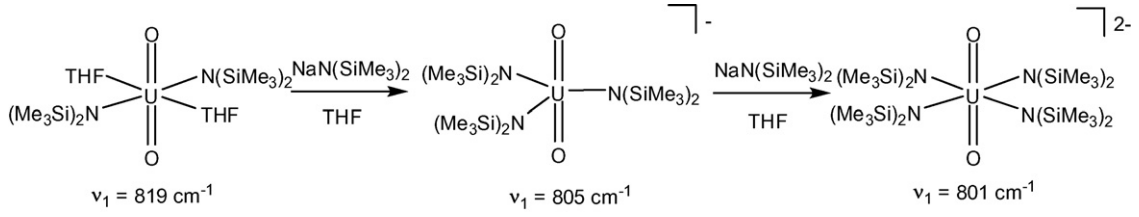

Scheme 1.

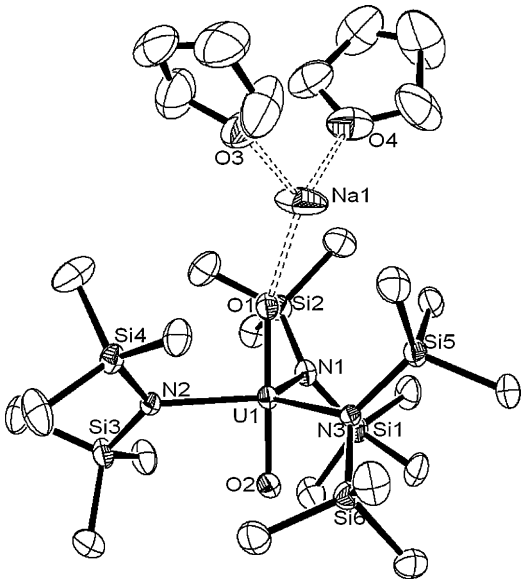

Fig. 4. Solid-state molecular structure of $[Na(THF)_2][UO_2(N(SiMe_3)_2)_3]$ taken from Ref. [44].

is clearly demonstrated in $[UO_2(N(SiMe_3)_2)_n]^{2-n}$ (n = 2–4). Successive addition of the silylamide ligands to the uranyl ion leads to a decrease in the U=O symmetric stretching frequency (ν_1), from 819 cm^{-1} in the bis(amido), to 805 cm^{-1} in the tris(amido), to 801 cm^{-1} in the tetrakis(amido) (Scheme 1) [44].

This weakening leads to an enhancement of oxo ligand basicity, reflected by the formation of the $O_{yl} \rightarrow Na$ interaction in the solid-state molecular structure of $[Na(THF)_2][UO_2(N(SiMe_3)_2)_3]$ (Fig. 4) [44]. The coordination environment of the sodium cation in this complex consists of two THF molecules and one uranyl oxo, affording a trigonal pyramid geometry. In addition, the presence of a Na–C contact reveals that one of the silylamide methyl carbons is weakly coordinated to the cation. The coordination of Na to the uranyl oxo is also reflected in the U=O bond lengths, as the sodium bound U–O_{yl} distance (1.810(5) Å) is slightly longer than the terminal U–O_{yl} distance (1.781(5) Å) [44]. This structural perturbation is a common consequence of $O_{yl} \rightarrow M$ interactions [10,40], and may serve to activate U=O bonds to further functionalization. Indeed, coordination of potassium to an "yl" oxygen atom has been implicated as a key step in the reductive silylation of uranyl (see Section 4.2) [45].

Similar uranyl–cation interactions have also been observed in the solid-state molecular structures of the uranyl benzaminato complexes $[Na(THF)_2PhCN][UO_2(NCN)_3]$ and $[Na(THF)UO_2(NCN)_2]_2(\mu_2\text{-}O)$ ($NCN^- = PhC(NSiMe_3)_2^-$) [10]. The U–O_{yl} bond lengths in $[Na(THF)_2PhCN][UO_2(NCN)_3]$, are unsymmetrical (e.g., U–O_{yl} = 1.783(3) and 1.812(3) Å) due to the interaction of the "yl" oxygen with the sodium cation [10], while the uranyl symmetric stretching frequencies for $[Na(THF)_2PhCN][UO_2(NCN)_3]$ (ν_1 = 773 cm^{-1}) and $[Na(THF)UO_2(NCN)_2]_2(\mu_2\text{-}O)$ (ν_1 = 757 cm^{-1}) are also indicative of functionalized U=O bonds, being much lower than most uranyl complexes (*cf.* $[UO_2Cl_2(THF)_2]_2$, ν_1 = 834 cm^{-1}) (Scheme 2) [10]. NMR analysis of $[Na(THF)_2PhCN][UO_2(NCN)_3]$ in C_6D_6 is consistent with the $O_{yl} \rightarrow Na$ interactions being largely maintained in solution, as only small amounts of $UO_2(NCN)_2(THF)$ and free Na[NCN] are present.

The enhanced nucleophilicity of the uranyl oxo ligands, arising from the electron donation of the equatorial NCN ligands, was further illustrated by the addition of $B(C_6F_5)_3$ to $UO_2(NCN)_2(THF)$, yielding $UO\{OB(C_6F_5)_3\}(NCN)_2$ (Eq. (1)) [38]. Several transition metal oxo-borane adducts are known [46–48], but $UO\{OB(C_6F_5)_3\}(NCN)_2$ is the first example of a uranyl complex functionalized by borane addition. The U–O bond distance of the borane-coordinated oxo (1.898(3) Å) is notably longer than the U–O bond length of the terminal oxo (1.770(3) Å) [38]. The difference is larger than that observed in $[Na(THF)_2PhCN][UO_2(NCN)_3]$, likely a result of the strong Lewis acidic character of $B(C_6F_5)_3$. The interaction with $B(C_6F_5)_3$ is also maintained in C_6D_6, as indicated by the Raman and ^{11}B NMR spectra. A second $B(C_6F_5)_3$-uranyl adduct has recently been reported, namely $UO(O\{BC_6F_5\}_3)(^{Ar}acnac)_2$ ($^{Ar}acnac = [ArNC(Ph)CHC(Ph)O]^-$, Ar = 3,5-$^tBu_2C_6H_3$) [49]. The formation of this complex is promoted by the use of an electron rich β-ketoiminate ligand ($^{Ar}acnac$), and its metrical parameters are similar to those observed for $UO\{OB(C_6F_5)_3\}(NCN)_2$.

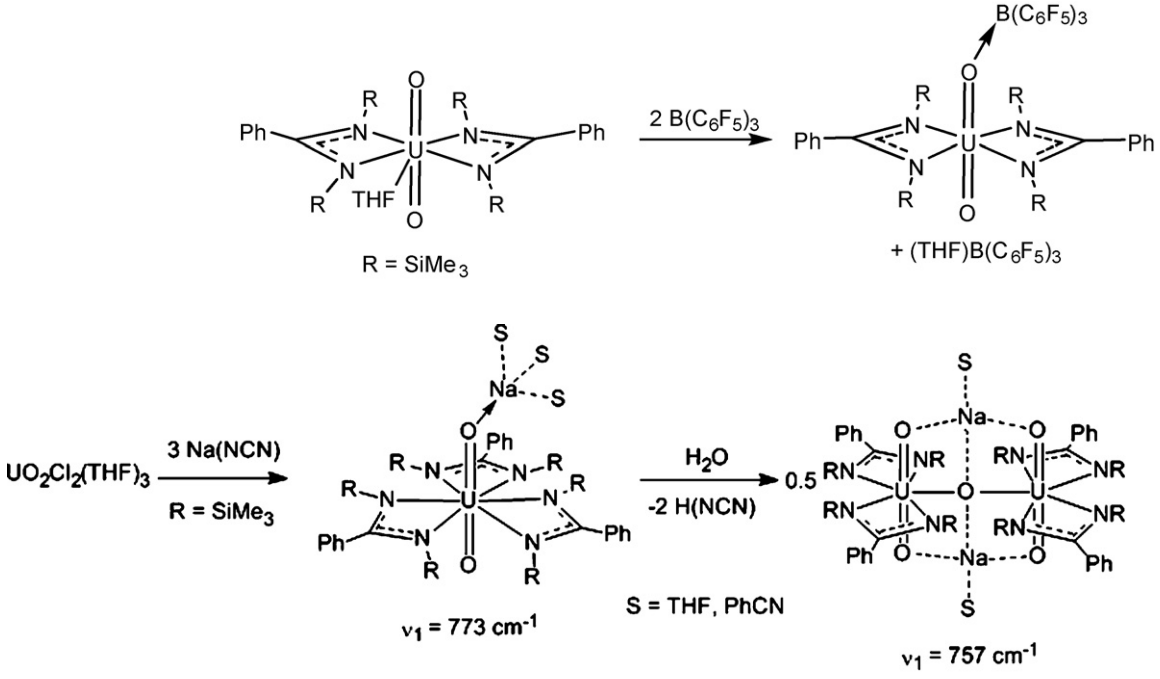

Scheme 2.

Coordination of a uranyl oxo ligand to a transition metal ion has also been observed. For instance, complexation of uranyl by a Schiff-base pyrrole-immine macrocycle, followed by addition of a 3d transition metal results in the generation of a "Pac-Man" topology and formation of a $O_{yl} \rightarrow M$ (M = Mn, Fe, Co) bond (Eq. (2)) [40,45,50]. As anticipated, the U–O_{yl} bond of the bridging oxo ligand is lengthened relative to the terminal U=O bond. In the case of manganese, the bridging U–O_{yl} bond distance is 1.808(4) Å, which is longer than the terminal U–O_{yl} bond length of 1.768(5) Å [40]. This mode of coordination is enhanced by the geometrical constraints of the ligand but also through the strongly σ-donating imino and pyrrolide groups. In fact, these complexes exhibit ν_1 stretching frequencies of 811, 804, and 807 cm^{-1}, for Mn, Fe, and Co, respectively [40], which are comparable to those observed for $[UO_2(N(SiMe_3)_2)_n]^{2-n}$ (n = 2–4) [44], and $[Na(THF)_2PhCN][UO_2(NCN)_3]$ [10].

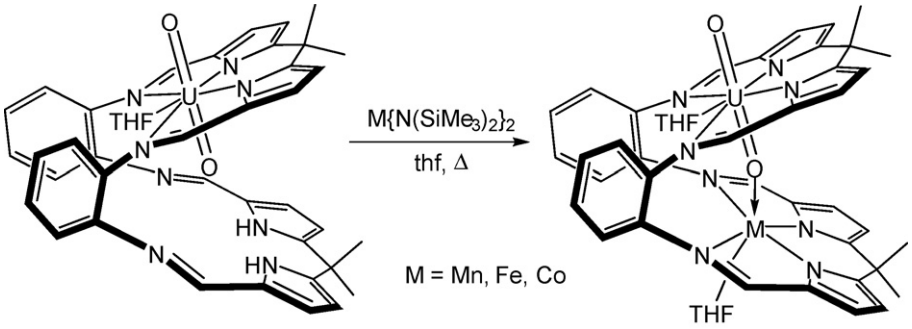

(2)

Uranyl–cation interactions are not limited to N-donor ligand sets and they have also been observed in the solid-state molecular structures of a uranyl aryloxide $[Na(THF)_3]_2[UO_2(O\text{-}2,6\text{-}Me_2C_6H_3)_4]$ [51], uranyl calixarenes [52–55], uranyl oxalates [56,57], a uranyl carboxylate [58], and a uranyl salophen complex [59,60]. The uranyl halides, $[Na(15\text{-crown-}5)]_2[UO_2Br_4]$ and $[Li(12\text{-crown-}4)]_2[UO_2X_4]$ (X = Cl, Br) [61], also exhibit $O_{yl} \rightarrow M$ interactions (Scheme 3). Interestingly, the analogous potassium salts do not exhibit a cation interaction with the "yl" oxygen atoms. This observation was rationalized by invoking HSAB theory [61]. A weak interaction between NO^+ and uranyl has also been observed in the solid-state molecular structure of $[NO][UO_2(NO_3)_3]$ [62], however disorder of the nitrosonium cation precludes accurate assessment of the $O_{yl} \rightarrow NO^+$ distances.

3.2. Uranyl–cation interactions in extended solids

Because of their importance in the nuclear fuel cycle and in uranium speciation [63,64], hundreds of uranyl-containing complexes and minerals have been characterized by X-ray crystallography [65]. In the solid-state, the uranyl ion can accommodate up to six atoms in its equatorial plane, and commonly adopts square, pentagonal, and hexagonal bipyramidal geometries. Uranyl polyhedra can link through equatorial vertices, edges *and* the axial "yl" oxygen atoms to form extended solids [65]. In fact, interactions with the "yl" oxygen atoms and metal cations, $O_{yl} \rightarrow M$, are reasonably common in these materials. For instance, the simple metal uranates (which contain the UO_2^{2+} ion), such as Li_2UO_4 [66], Na_2UO_4 [67], $K_2U_2O_7$ [68], and MUO_4 (M = Mg, Ca, Sr, Ba) [69–71], each display $O_{yl} \rightarrow M$ contacts with their respective alkali and alkaline earth counterions. Similar interactions are also found in a number of other uranyl materials (e.g., $K(H_2O)[(UO_2)_3(\mu_3\text{-}OH)(\mu_2\text{-}OH)(C_7H_4O_4N)_2]$, $C_7H_4O_4N$ = *p*-nitrobenzoate) [72,73], and several minerals [74–78]. While these interactions are weak (judging by the $O_{yl} \rightarrow M$ distances) they can serve as linkers between uranyl polyhedral, allowing for the assembly of unique topologies. For instance, these linking interactions are found in the solid-state molecular structure of $\{Li(H_2O)_2[(UO_2)_2Cl_3(O)(H_2O)]\}_n$, where the $O_{yl} \rightarrow Li$ interactions connect separate uranyl polyhedral sheets to build a 3D framework (Fig. 5) [76].

Bridging interactions of the "yl" oxygen atoms in extended solids are not limited to the Group 1 and 2 metals. $O_{yl} \rightarrow M$ contacts have also been observed with transition metals and main group elements, such as Ag^+ [79], Cu^{2+} [80–82], Zn^{2+} [83], Co^{2+} [84], and Pb^{2+} [85].

3.3. Hydrogen bonding in uranyl

The uranyl "yl" oxygen atoms can also act as hydrogen bond acceptors [4,39,41,86–96], and these interactions have been observed in the solid-state molecular structures of many uranyl-containing materials [88,97], including $UO_2Cl_2{\cdot}H_2O$ [86], $[UO_2(SO_4)(OH_2)_2]_2{\cdot}$(benzo-15-crown-5)$\cdot 3H_2O$ [87], $[C(NH_2)_3]_6[(UO_2)_3(CO_3)_6]\cdot 6.5H_2O$ [41], $[Co(NH_3)_6]_2[UO_2(OH)_4]_3\cdot H_2O$ [39], and $[Hpyr]_2[UO_2(L)]\cdot 3H_2O$ (where pyr = pyrrolidine and L = *p*-*tert*-butyl-

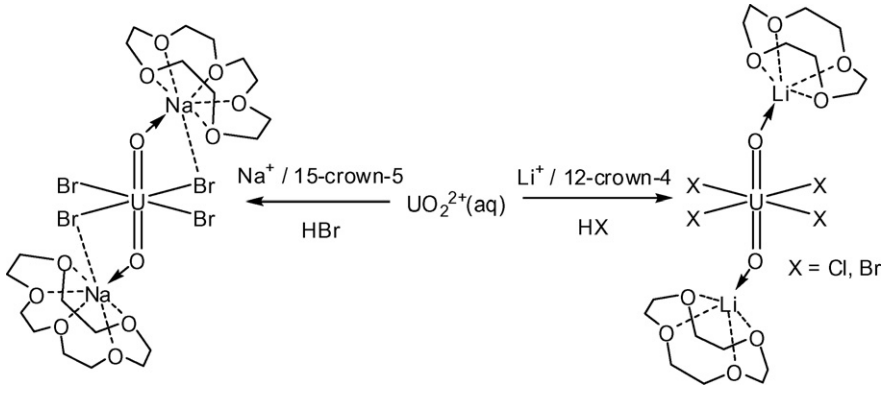

Scheme 3.

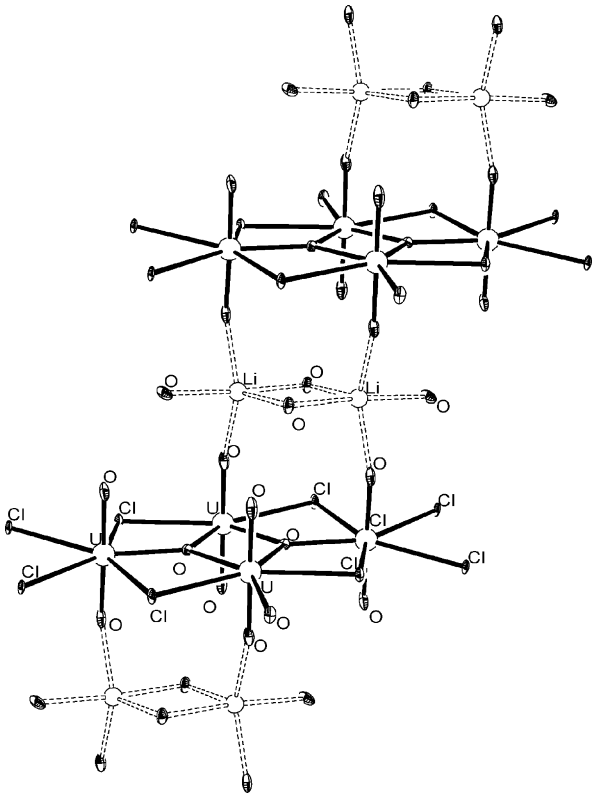

Fig. 5. Uranyl polyhedral sheets of $\{Li(H_2O)_2[(UO_2)_2Cl_3(O)(H_2O)]\}_n$ linked by $O_{yl} \rightarrow Li$ contacts. Taken from Ref. [76].

but extremely weak [102]. However, a hydrogen bonding interaction is predicted for the pentavalent analogue, $[UO_2(H_2O)_5]^+$, which exhibits a larger negative charge on its "yl" oxygens than that observed for uranyl(VI) [98].

Hydrogen bonding with the uranyl oxo ligands has also been observed in several biological systems. Uranyl is sometimes added as a heavy atom source for protein crystallography, and the uranyl oxo ligands are often found to be involved in hydrogen bonding with the amino acid side chains of proteins [4]. For example, in the glycoprotein N-cadherin NCD1, hydrogen bonding occurs between uranyl oxo ligands and the N–H amide protons of the peptide backbone and an asparagine side chain [4,103].

The hydrogen bond accepting capabilities of uranyl have also been utilized in the development of novel ligands which exploit the rigid geometry of the uranyl fragment. These ligands possess several coordinating groups built around a central hydrogen bond donor to generate a cavity that encapsulates the uranyl fragment by equatorial coordination *and* by hydrogen bonding to the oxo group [88,89]. This molecular recognition approach generates ligands with high specificity for uranyl. For instance, the tripodal ligand tris[3-(2-carboxy-4-octadecylphenoxy)propyl]amine (NPodB) strongly complexes the uranyl ion with three carboxylate-containing arms (Eq. (3)) [88]. The NPodB ligand also contains a tertiary amine which, when protonated with HCl, provides a proton for a hydrogen bond interaction with the "yl" oxygen. Although these complexes have not been structurally characterized, mass spectrometry supports formation of a 1:1 complex, while vibrational spectroscopy is consistent with the presence of a hydrogen bonding interaction. These "stereognostic" ligands exhibit extraction coefficients ranging from $\sim 10^{11}$ to $\sim 10^{14}$ at neutral pH [88,89].

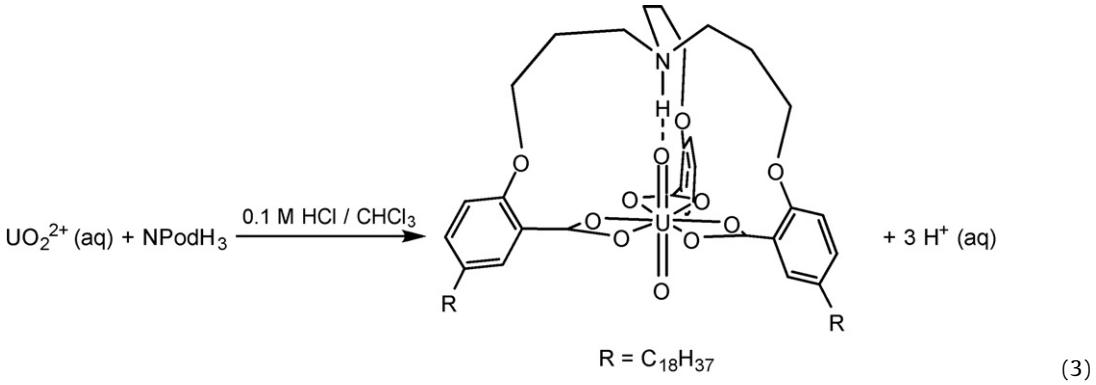

(3)

tetrahomodioxacalix[4]arene) [90]. Hydrogen bonding does not appear to disrupt the U=O bonds as significantly as does the coordination of metal cations, and the metrical parameters of the uranyl fragment in these complexes are usually normal. Hydrogen bonding interactions have also been observed in the solid-state molecular structure of the uranyl Pac-Man pyrrole-immine macrocycle (*vide supra*) in the absence of a transition metal [91]. The interaction occurs between the *endo* "yl" oxygen atom and two pyrrolic hydrogen atoms. In this case, only a small, but detectable, change is observed in the U–O bond length (e.g., bridging U–O_{yl} = 1.790(4) Å, terminal U–O_{yl} = 1.766(4) Å). Because of the ligand architecture, the hydrogen bonding interactions are conserved in solution, as indicated by ^{1}H NMR spectroscopy [91].

Computational studies suggest that H-bonding between the "yl" oxygens of $[UO_2(H_2O)_5]^{2+}$ and bulk water either does not occur [98,99], or is rather weak [100,101], depending on the level of theory used. Similarly, calculations reveal that a hydrogen bond between the "yl" oxygen in $[UO_2(H_2O)_5]^{2+}$ and methanol is present

3.4. Uranyl(V)–cation interactions

While there are only a few well defined UO_2^+ complexes, several of these exhibit $O_{yl} \rightarrow M$ interactions. For example, the coordination of potassium to an oxo ligand is observed in the solid-state molecular structure of the 1-D coordination polymer $\{[UO_2(Py)_5][KI_2(Py)_2]\}_x$ [2,3,13,14]. Similarly, interactions between the uranyl(V) oxo ligands and potassium have been observed in $\{[UO_2(dbm)_2]_2[\mu\text{-}K(Py)_2]_2[\mu_8\text{-}K(Py)]\}_2^{2+}$, $\{[UO_2(dbm)_2]_2[\mu\text{-}K(MeCN)_2][\mu_8\text{-}K]\}_2$ and $\{[K(18\text{-crown-6})][UO_2(dbm)_2]\}_2$ [16,104]. These complexes also exhibit "cation–cation interactions" between the uranyl fragments in the cluster (Section 3.5.2).

3.5. Uranyl cation–cation interactions

The coordination of an actinyl "yl" oxygen to the metal center of another actinyl fragment (e.g., $O_{yl} \rightarrow AnO_2^{n+}$), is commonly referred to as a cation–cation interaction (CCI). Actinide CCI's are integral to

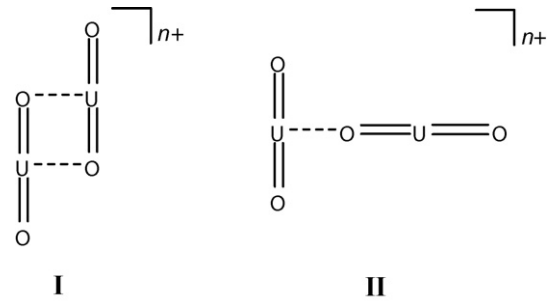

Fig. 6. Uranyl cation–cation interactions (CCIs) with side-on (**I**) and end-on (**II**) coordination.

understanding the solution and solid-state behavior of the actinyl ions and have been identified in UO_2^{2+} and AnO_2^{+} (An = U [105], Np [106–111], Pu [112,113], Am [114]). The prevalence of CCI's is highly dependent on the actinide involved. For instance, CCI's are relatively common for neptunyl(V) (NpO_2^{+}) [106,115], but are rarely observed for UO_2^{2+}. The discrepancy between NpO_2^{+} and UO_2^{2+} likely arises from the differences in Lewis basicity of their oxo ligands. The neptunium ion in NpO_2^{+} possesses a $5f^2$ electron configuration which increases the electrostatic repulsion between the metal and its oxo groups. In contrast, UO_2^{2+} has a $5f^0$ electron configuration and lacks this electrostatic interaction [6]. Nevertheless, a handful of uranyl-uranyl CCI's have been observed in the solid-state for uranyl(VI) [116–132], and these complexes are discussed in detail in the following section.

3.5.1. Uranyl(VI) cation–cation interactions

Uranyl complexes exhibiting cation–cation interactions (CCI's) can be broadly classified into two structural categories: a side-on doubly oxo-bridged structure (**I**) or an end-on singly oxo-bridged structure (**II**) (Fig. 6). The latter interaction is relatively flexible and can pivot at the coordinating "yl" oxygen, and U–O_{yl}–U angles from 177° [133] to 110° [122] have been observed in the solid-state. Structure **II** has also been probed by theoretical methods [134].

In the uranyl-containing uranium(VI) oxides, UO_3 and $UO_3{\cdot}H_2O$, the lack of ancillary ligands is compensated by the formation of CCI's with neighboring uranyl cations [116,120]. In the solid-state molecular structure of UO_3, each "yl" oxygen atom is involved in a side-on (**I**) CCI with an adjacent uranyl cation, and the observed $O_{yl} \rightarrow U$ distances are 2.38(2) and 2.56(2) Å [116]. Similar interactions are also observed in $UO_3{\cdot}H_2O$ [120]. Linking of uranyl polyhedra through CCI's has also been observed in the solid-state structures of UO_2Cl_2 (which exhibits structure **I**) [119], and β-UO_2SO_4 [117], α-UO_2SeO_4 [117], $(NH_4)_3(H_2O)_2\{[(UO_2)_{10}O_{10}(OH)][(UO_4)(H_2O)_2]\}$ [125], $M[(UO_2)_3(HIO_6)(OH)(O)(H_2O)]{\cdot}1.5H_2O$ (M = Li–Cs) [123], $Sr_5(UO_2)_{20}(UO_6)_2O_{16}(H_2O)_6$ [126], and $Cs(UO_2)_9U_3O_{16}(OH)_5$ (all of which exhibit structure **II**) [126]. These complexes form 3-D frameworks, with the exceptions of β-UO_2SO_4 and UO_2SeO_4, which form infinite chains. Their U–O_{yl} bonds are typically elongated relative to those observed in discrete uranyl complexes. For instance, the U–O_{yl} bond length for the bridging "yl" oxo in $Cs[(UO_2)_3(HIO_6)(OH)(O)(H_2O)]$ is 1.827(7) Å [123], slightly longer than the usual U–O_{yl} distance. However, the U–O_{yl} bonds for the bridging "yl" oxo ligands in $(NH_4)_3(H_2O)_2\{[(UO_2)_{10}O_{10}(OH)][(UO_4)(H_2O)_2]\}$ (av. 1.94 Å) [125], and $Sr_5(UO_2)_{20}(UO_6)_2O_{16}(H_2O)_6$ (1.87(1) and 1.967(9) Å) [126], exhibit a significant lengthening.

CCI's are not exclusive to extended solids and have been observed in discrete molecules in a few instances. For example, addition of hexafluoroacetylacetone (hfac) to $UO_3{\cdot}2H_2O$ yields the uranyl trimer $[UO_2(hfac)_2]_3$ [121,135]. The three monomer units in

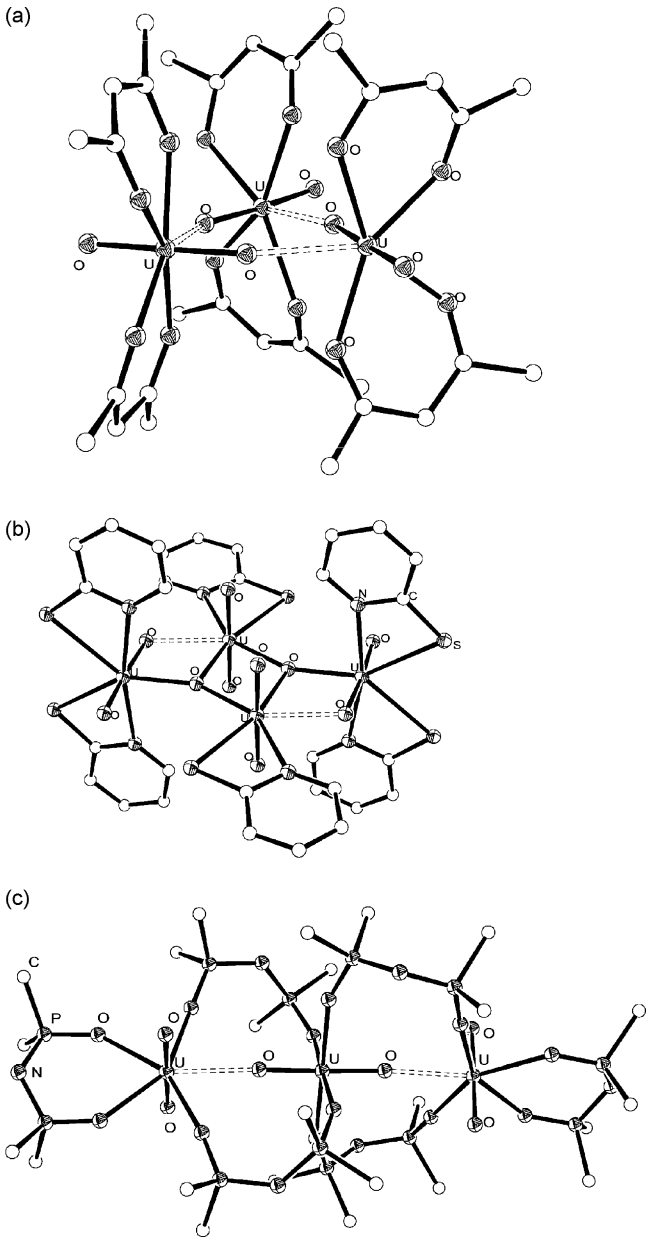

Fig. 7. Solid-state molecular structures of (a) $[UO_2(hfac)_2]_3$ (fluorine atoms removed for clarity), (b) $[NEt_3H]_2[(UO_2)_4(O)_2(o\text{-}S\text{-}C_5H_4N)_6]$, and (c) $[UO_2\{(OPPh_2)_2N\}_2]_3$ taken from Refs. [121,122,133], respectively. In (c) only the *ipso* carbons of the phenyl groups are shown.

$[UO_2(hfac)_2]_3$ are connected via end-on CCI's (structure **II**), where one oxo group from each uranyl cation acts as a bridge between metal centers (Fig. 7a) [121]. Due to the low precision of the structure, the bridging U–O_{yl} bond distances (av. 1.77 Å) and the terminal U–O_{yl} distances (av. 1.70 Å) [121], are identical by the 3σ criterion. The trimeric structure is broken apart in coordinating solvents, which can disrupt the CCI's [121].

Similarly, the tetrameric uranyl alkoxide complex $[UO_2(OCH(^iPr)_2)_2]_4$, synthesized by reaction of $UO_2Cl_2(THF)_3$ with $KOCH(^iPr)_2$ in THF, exhibits bridging, end-on CCI's (**II**) linking the four uranium centers [43]. The octahedral coordination environment of each uranyl cation in $[UO_2(OCH(^iPr)_2)_2]_4$ is completed by two bridging and one terminal diisopropylmethoxide groups. As anticipated, the bridging U–O_{yl} bond length (1.846(4) Å) is longer than the non-bridging U–O_{yl} bond (1.783(4) Å) [43]. According to NMR spectroscopy, the tetramer is maintained

in C_6D_6 solutions but exists in equilibrium with $UO_2(OCH(^iPr)_2)_2L_2$ (L = Lewis base) in polar solvents such as THF.

In the uranyl oxo thiolate complex $[HNEt_3]_2[(UO_2)_4(\mu_3\text{-}O)_2(o\text{-}S\text{-}C_5H_4N)_6]$ (o-S-C_5H_4N = 2-thiopyridyl), CCI's also act to form a tetrameric assembly [122]. Each uranyl cation possesses a pentagonal bipyramidal coordination environment. However, only the oxo groups of two uranyl cations are involved in end-on CCI's (**II**), as illustrated in Fig. 7b.

Incorporation of uranyl cations into *p*-benzylcalix[7]arene in the presence of 1,4-diazabicyclo[2.2.2]octane (DABCO) also yields a uranyl CCI complex [124]. This complex, $(UO_2)_6(L)_2(O)_2(HDABCO)_6$, (L = *p*-benzylcalix[7]arene), contains a hexametallic uranyl cluster where two of the six uranyl moieties exhibit end-on CCI's.

Another molecule which exhibits CCI's is the trimetallic complex $[UO_2\{(OPPh_2)_2N\}_2]_3$, formed by addition of $K[N(Ph_2PO)_2]$ to $UO_2(NO_3)_2$ [133]. Its solid-state molecular structure consists of two uranyl cations linked by a bridging UO_2^{2+} fragment via two end-on CCI's (**II**), U ← O_{yl}=U=O_{yl} → U (Fig. 7c). Despite the involvement of the central uranyl cation in the CCI's, minimal distortion of the O=U=O bonds is observed, as the bridging U–O_{yl} bond distances (1.793(4) Å) are only slightly longer than the terminal U–O_{yl} distances (av. 1.739 Å) [133].

3.5.2. Uranyl(V) cation–cation interactions

Reduction of UO_2^{2+} to UO_2^{+} confers a higher degree of Lewis basicity upon the "yl" oxygen atoms, promoting the formation of CCI's. However, CCI's may provide a facile pathway for disproportionation of uranyl(V) to UO_2^{2+} and U^{4+} [136], making the isolation of this class of materials particularly challenging. This difficulty was overcome by Mazzanti and coworkers, who isolated a series of uranyl(V) complexes, each containing CCI's [104]. The solid-state molecular structures of $\{[UO_2(dbm)_2]_2[\mu\text{-}K(Py)_2]_2[\mu_8\text{-}K(Py)]\}_2\cdot 2I\cdot 2Py$ and $[UO_2(dbm)_2K(18\text{-crown-}6)]_2$ both possess CCI's in the solid-state, while an NMR analysis indicates that the CCI's are preserved in THF solutions. However, addition of stronger donors, such as pyridine or DMSO, results in formation of monomeric complexes (e.g., $K[UO_2(dbm)_2(DMSO)]$) [104]. A more thorough description of this chemistry can be found in recent reviews by Arnold [3] or Kiplinger [2]. The stabilization and isolation of these complexes may have technological implications as they could be employed to model the behavior of the highly radioactive neptunyl ions which are present in spent nuclear fuel [104].

4. Synthetic approaches for U–O bond cleavage

The activation, functionalization, and substitution chemistry of transition metal oxo complexes is well established. These metal systems are often employed in catalysis and as oxo transfer reagents [137–143]. In contrast, the uranyl cation does not exhibit this behavior, and only a few examples of oxo functionalization and/or substitution are known for uranyl. However, a number of recent reports have demonstrated that controlled disruption of the $[O=U=O]^{2+}$ fragment is possible and these novel complexes represent an emerging area of actinide chemistry.

4.1. Uranyl oxo substitution

The coordination of aryloxides to uranyl is known to weaken the U=O bonds, thereby promoting the formation of O_{yl} → M interactions (as observed in the solid-state molecular structure of $[Na(THF)_3]_2[UO_2(O\text{-}2,6\text{-}Me_2C_6H_3)_4]$ [51]). In contrast, the coordination of alkoxides, which are stronger donors than aryloxides [144], can induce a different mode of reactivity: oxo ligand scrambling [43,145–147]. For example, addition of the strong σ-donating *tert*-butoxide ligand, $^tBuO^-$, to UO_2Cl_2 in THF leads to the formation of $[UO_2(O^tBu)_2][UO(O^tBu)_4]_2$ in 30% yield (Scheme 4). This complex results from formal substitution of O^{2-} by 2 equiv. of $^tBuO^-$, generating "$UO(O^tBu)_4$". This species is subsequently trapped by $UO_2(O^tBu)_2$ [146]. An insoluble precipitate is formed during the course of the reaction, which is likely "$UO_3(THF)_x$", whose formation accounts for the missing oxo ligands. In the solid-state $[UO_2(O^tBu)_2][UO(O^tBu)_4]_2$ contains two asymmetrically bridged oxo ligands, with U–O_{oxo} bond lengths of 1.923(6) Å and 2.301(6) Å. The latter interaction is comparable to the bridging *tert*-butoxide distance of 2.378(6) Å [146]. This complex is likely formed via a CCI-containing intermediate, as evidenced by the isolation of the tetrameric uranyl alkoxide $[UO_2(OCH(^iPr)_2)_2]_4$ (*vide supra*) [43]. Interestingly, addition of $OPPh_3$ during the course of the reaction results in the sole formation of $UO_2(O^tBu)_2(OPPh_3)_2$, which is stable to oxo ligand scrambling, possibly because it is unable to form CCIs [146].

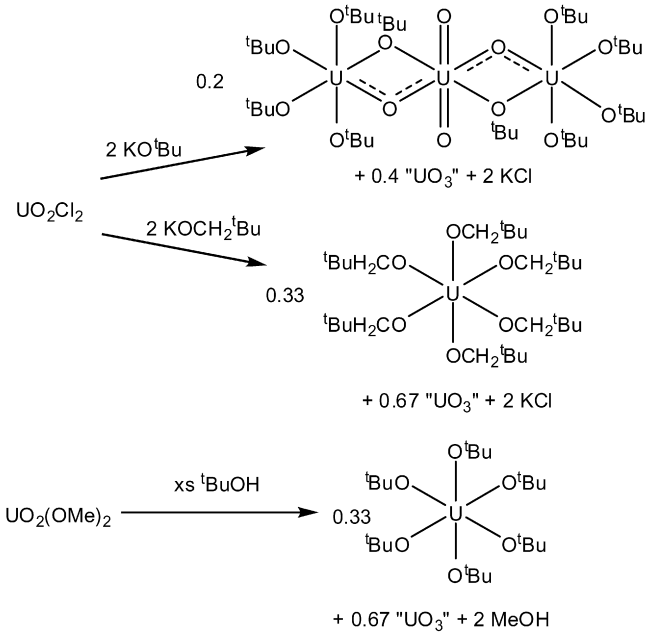

Scheme 4.

Similar reactivity is also observed upon reaction of $KOCH_2{}^tBu$ with $[UO_2Cl_2(THF)_2]_2$. This results in the formation of the homoleptic uranium(VI) alkoxide $U(OCH_2{}^tBu)_6$ in low yield (Scheme 4) [43]. The formation of $U(OCH_2{}^tBu)_6$ is likely due to oxo ligand scrambling, which generates "UO_3" as a by-product [43]. The formation of $U(O^tBu)_6$ by alcoholysis of $UO_2(OMe)_2$ with ^tBuOH probably occurs in a similar fashion (Scheme 4) [145]. However, it should be noted that addition of alkoxides to uranyl does not always elicit oxo ligand exchange. For instance, $UO_2(OCHPh_2)_2(THF)_2$ does not undergo this type of reactivity, possibly because its alkoxide ligands are not sufficiently electron-donating [43].

Complexation of $[HNC_5H_5]_2[UO_2Cl_4]$ with ^{t}Bu-calix[6]arene and $La(OTf)_3$ results in the surprising substitution of both U=O bonds, resulting in the formation of a uranium(VI) aryloxide in low yield [147]. The complex produced, $U[(H_2L)LaCl_2(Py)_4]_2$, (L = ^{t}Bu-calix[6]arene), possesses an octahedral uranium(VI) atom ligated by three phenolate oxygens from each calix[6]arene (Eq. (4)). Further analysis of the reaction mixture provided crystals of the uranium oxide cluster $[ULa_9O_8Cl_{15}(OTf)_6(Py)_9]^{4-}$ [147]. This complex possesses a "UO_6" core with each oxygen atom additionally coordinating three lanthanum cations. The oxo ligands in this complex are likely those displaced from $[UO_2Cl_4]^{2-}$ during the formation of

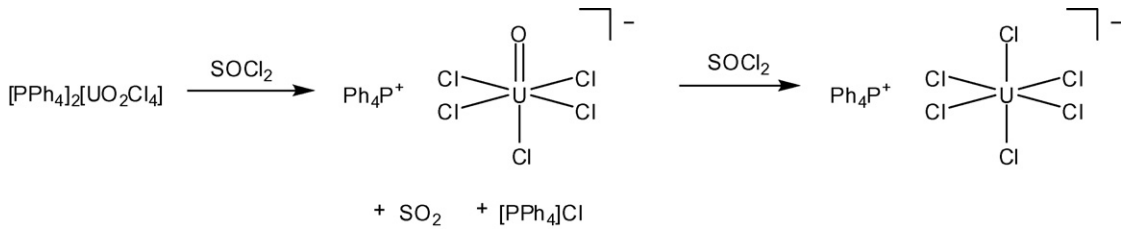

Scheme 5.

$U[(H_2L)LaCl_2(Py)_4]_2$. In contrast, the use of CsOTf in place of lanthanum did not lead to oxo ligand substitution. Instead, a uranyl calix[6]arene complex with long $O_{yl} \rightarrow Cs$ interactions was isolated [148].

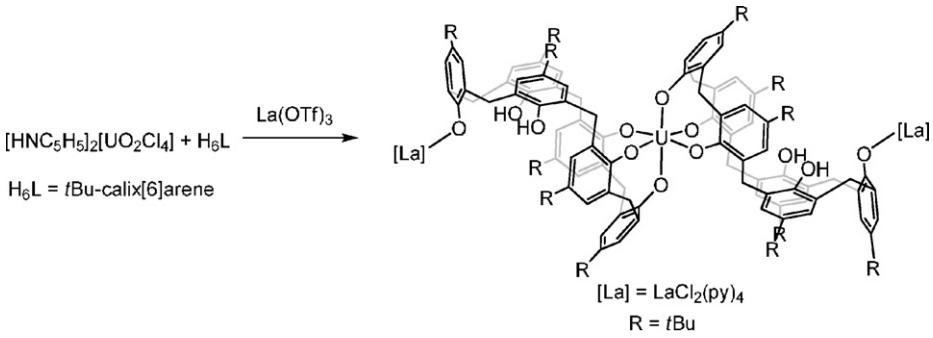

(4)

An attempt to synthesize a *cis* uranyl complex by coordination of a tripodal triamidoamine ligand to uranyl, lead to the unexpected isolation of a mixed-valent uranium(V/VI) oxo-imido dimer $[K(18\text{-crown-6})(Et_2O)_2][UO(\mu_2\text{-}NCH_2CH_2N(CH_2CH_2NSi^tBuMe_2)_2]_2$ (Eq. (5)) [149]. The complex, which can be isolated in 44% yield, is generated by elimination of a silyl group from an amido nitrogen, loss of an oxo ligand, and $1e^-$ reduction; however the exact mechanism of its formation is unknown [149]. The imido group bridges the two uranium ions producing a complex reminiscent of the side-on CCI's observed for uranyl (i.e., structure **I**).

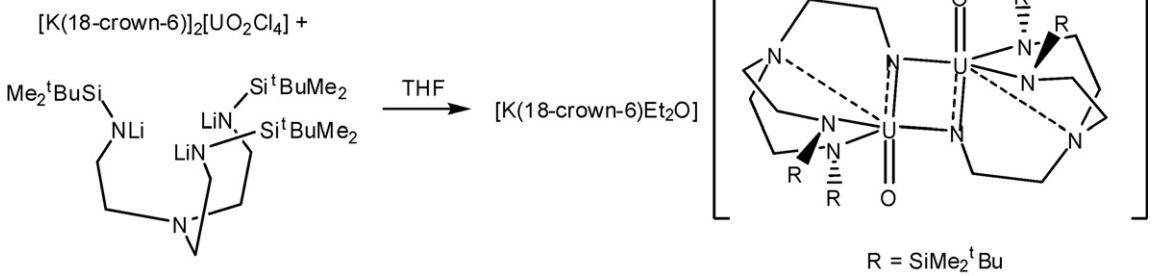

(5)

Another interesting example of oxo ligand substitution in uranyl is the deoxygenation of $[PPh_4]_2[UO_2Cl_4]$ with thionyl chloride (Scheme 5) [150–152]. This provides $[PPh_4][UOCl_5]$, which spontaneously deposits out of the reaction mixture as red crystals in good yields. Interestingly, only the PPh_4^+ salt is known, and its successful isolation depends on its precipitation from the reaction mixture, as longer reaction times lead to the formation of the U(V) complex, $[PPh_4][UCl_6]$. Interestingly, when NEt_4^+ was used as a counterion, only $[NEt_4][UCl_6]$ was isolated [151].

4.2. Reductive functionalization of uranyl oxo ligands

The reductive silylation of a uranyl oxo ligand, reported by Arnold et al. [45], has been recently reviewed [2,3]. In contrast to this example, complete deoxygenation of uranyl can be achieved by addition of excess Me_3SiX (X = Cl, Br, I) to $UO_2I_2(THF)_3$ or $UO_2(OTf)_2$ in MeCN. This results in complete substitution of both oxo ligands, affording the U(IV) tetrahalides, $UX_4(MeCN)_4$, in good yields (Eq. (6)) [153]. $Me_3SiOSiMe_3$ is the likely by-product, although it was not observed in the reaction mixture, while the driving force for this reaction is probably the formation of strong Si–O bonds.

$$UO_2I_2(THF)_3 + 3\,Me_3SiX \xrightarrow[X=Cl,\,Br,\,I]{MeCN} UX_4(MeCN)_4 \quad (6)$$

The functionalization of the uranyl fragment has also been accomplished through reduction with U(III) [154]. Thus, treatment of $UO_2(OTf)_2$ with $U(OTf)_3$ in pyridine/MeCN affords the U(IV) oxide cluster $[U_6(\mu_3\text{-}O)_8(\mu_2\text{-}OTf)_8(Py)_8]$ in 85% yield. The structural features of the uranyl moiety are not preserved upon reduction, as indicated by the long U–O(oxo) bond lengths (av. 2.25(3) Å) [154].

4.3. Light-mediated functionalization of uranyl

The uranyl ion exhibits a long-lived triplet excited state, abbreviated $^*UO_2^{2+}$, which is accessible by exposure to sunlight [155]. The excited state of uranyl is a powerful oxidant, with a redox potential of 2.6 V, on par with F_2 [156]. In line with this potential, $^*UO_2^{2+}$ can abstract hydrogen from alcohols [157], alkanes [158,159], arenes [160], and alkenes [161]. However, its photochemical properties also provide a pathway for uranyl functionalization. For instance, the light-mediated reduction of uranyl-oxalate to $U^{IV}O_2$, with concomitant generation of CO_2, is extremely efficient at

low pH [162]. In fact, uranyl(VI) oxalate is often used as a chemical actinometer [163]. Similarly, photolysis of $[UO_2(OPPh_3)_4][OTf]_2$ in the presence of MeOH or Et_2O results in the formation of the U(IV) alkoxides $[U(OMe)_2(OPPh_3)_4][OTf]_2$ and $[U(OEt)_2(OPPh_3)_4][OTf]_2$, respectively (Scheme 6) [164]. The reduction is postulated to occur via oxidation of MeOH by $^*UO_2^{2+}$ which generates UO_2^+ and an α-hydroxy radical [102,164]. The α-hydroxy radical is then capable of reducing a second equivalent of UO_2^{2+}. Subsequent disproportionation of UO_2^+ generates the U(IV) product (and UO_2^{2+}). The process proceeds similarly with Et_2O, via initial formation of ethanol through C–O bond cleavage and H-atom abstraction [164]. Interestingly, the formation of U(IV) is reversible and addition of a H_2O/MeCN solution to $[U(OR)_2(OPPh_3)_4][OTf]_2$ (R = Me, Et) regenerates $[UO_2(OPPh_3)_4][OTf]_2$ (Scheme 6) [164]. $[UO_2(DPPMO_2)_2(Ph_3PO)][BF_4]_2$ ($DPPMO_2 = CH_2\{Ph_2PO\}_2$) can also be reduced by photolysis in MeOH [165]. The resulting product, $[U(DPPMO_2)_3F_2][BF_4]_2$, is isolable in 37% yield and is formed by fluoride abstraction from the BF_4^- moiety. Oxidation of this complex back to hexavalent uranyl is also possible with the use of moist air.

The photochemical reduction of uranyl has also been utilized to produce a series of uranium(IV) perrhenato complexes [166]. $[U(ReO_4)_4L_4]$ (L = tri-*n*-butylphosphine oxide, triethyl phosphate, tri-*iso*-butylphosphate) was synthesized by exposing an ethanol solution of $[UO_2(ReO_4)_2{\cdot}H_2O]$ to sunlight in the presence of the corresponding ligand [166].

An attempt to synthesize a phosphine sulfide adduct of uranyl also resulted in the isolation of a U(IV) complex [167]. Addition of NaS_2PMe_2 and Ph_3PS to $UO_2Cl_2{\cdot}3H_2O$ yields small amounts of $[U(S_2PMe_2)_2(O(S)PMe_2)(\mu\text{-}O_2PMe_2)]_2$ (Eq. (7)) [167]. Each uranium atom in $[U(S_2PMe_2)_2(O(S)PMe_2)(\mu\text{-}O_2PMe_2)]_2$ possesses a pentagonal bipyramidal geometry, where four sulfurs and one oxygen atom occupy the equatorial plane, and one $^-O(S)PPh_2$ ligand occupies an axial site. The second axial site is occupied by the bridging $^-O_2PMe_2$ ligand. The geometry of the complex suggests that the oxygen atoms in the $^-O(S)PPh_2$ ligands may have been derived from the uranyl oxo ligands [167], but it is possible that water is also an oxygen source. The reduction is thought to be light mediated, and is suspected to generate elemental sulfur as a by-product [167].

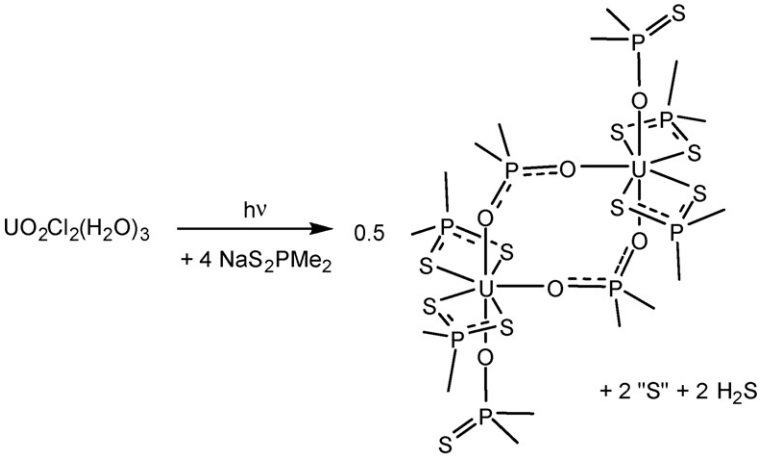

(7)

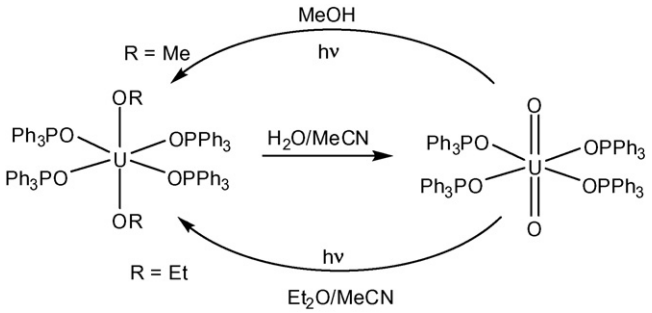

Scheme 6.

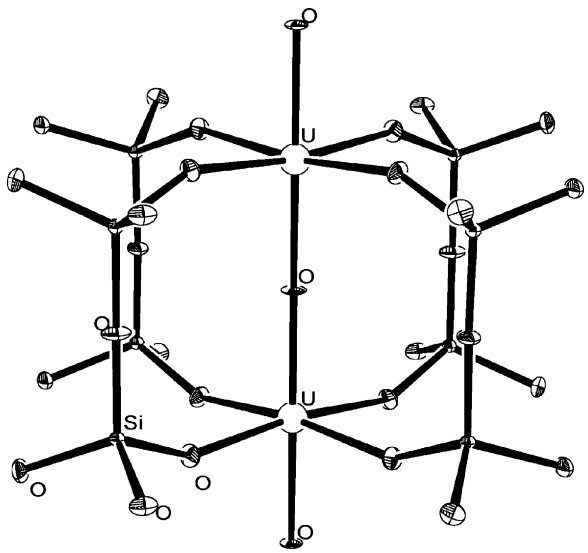

Fig. 8. Portion of the solid-state molecular structure of $\{K(UO)Si_2O_6\}_x$ (potassium cations removed for clarity) taken from Ref. [176].

4.4. Hydrothermal reduction of uranyl

The reduction of uranyl under hydrothermal conditions is well established [168–179], and by carefully tailoring the reaction conditions, cleavage of the $U–O_{yl}$ bonds can be effected to afford extended solids containing both U(IV) [168–174,179] and U(V) [176–178]. For example, hydrothermal treatment of uranyl and nickel acetate, in the presence of HF, at 200 °C results in the formation of the U(IV) fluoride complexes $\{Ni(H_2O)_4UF_6{\cdot}1.5H_2O\}_n$ and $\{Ni(H_2O)_2UF_6(H_2O)\}_n$ in 62% and 12% yields, respectively [179]. The reduction is believed to occur through decarboxylation of the acetate ligand. Indeed, the reducing agents in these hydrothermal reductions are often attributed to the organic templating ligands present in the system [179,180].

Substitution of the uranyl oxo groups upon hydrothermal reduction is not always complete and the $U–O_{yl}$ bonds can sometimes be retained. For instance, the novel pentavalent-uranium silicate

$\{K(UO)Si_2O_6\}_x$ consists of an octahedral U^{5+} cation coordinated by six oxygen atoms in an extended 3-D framework (Fig. 8) [176]. The uranium cation exhibits two U–O(oxo) bond lengths of 2.060(2) Å and 2.070(2) Å and four U–O(SiO) distances of 2.164(2) Å [176]. The uranium cations are linked via the bridging oxo ligand. The material was produced by hydrothermal treatment of UO_3 with an aqueous mixture of KOH, KF, and SiO_2 at 600 °C, and water is postulated to act as the reducing agent [176]. The addition of fluoride to the reaction mixture is believed to stabilize the proposed UO_2^+ intermediate and promote precipitation of the U(V) silicate [176]. Adjusting the reaction stoichiometry has also resulted in the formation of the related U(V) 3-D framework $K_3(U_3O_6)(Si_2O_7)$ [177].

In contrast to the reductive functionalization described above, there are several compounds, including $(NH_4)_3(H_2O)_2\{[(UO_2)_{10}O_{10}(OH)][(UO_4)(H_2O)_2]\}$ and $Sr_5(UO_2)_{20}(UO_6)_2O_{16}(H_2O)_6$ [125,126], which exhibit non-uranyl U^{6+} ions in their solid-state structures. For instance, in $Sr_5(UO_2)_{20}(UO_6)_2O_{16}(H_2O)_6$, one uranium ion is coordinated by four bridging oxo ligands (with U–O bond lengths of 1.99(1) Å and 2.01(1) Å) and two bridging hydroxide ligands (with a U–O bond length of 2.25(1) Å) [126]. This coordination geometry deviates significantly from that expected for uranyl. However, the mechanism by which these ions are formed is not known.

4.5. Microbial reduction of uranyl

The uranyl cation is highly water soluble and exhibits appreciable mobility in the environment, especially when complexed to ions such as carbonate. This mobility has lead to contamination of groundwater at numerous sites, including waste treatment and storage facilities [181–183]. A variety of methods have been developed to remediate these contaminated areas. For example, the relatively arduous 'pump-and-treat' technique involves extraction of large volumes of contaminated groundwater followed by a number of extensive purification processes [183]. However, a growing body of literature suggests that microbes may facilitate environmental cleanup by reducing the soluble UO_2^{2+} cation to insoluble UO_2 *in situ* [181,182,184–188]. This represents a cost effective and low-tech alternative for uranium remediation [182,187].

The mechanism of microbial uranyl redox conversion is not understood, and there have been several attempts, both by experimentalist and theorists, to elucidate this transformation [185,189]. In the absence of any other metals, microbes such as *Geobacter metallireducens*, *Alteromonas putrefaciens*, and *Geobacter sulfurreducens*, carry out acetate (or formate, lactate, pyruvate) oxidation utilizing uranyl as the terminal electron acceptor [184]. The mechanism of reduction has been explored by X-ray absorption spectroscopy [185]. Analysis of uranyl solutions incubated with *G. sulfurreducens* in the absence of light indicates a quick consumption of the UO_2^{2+} with a concomitant increase in UO_2^+. Interestingly, at short reaction times UO_2 itself is not observed [185], and is only formed gradually over the course of several hours. This suggests that the reduction to U(IV) is independent of the microbial activity [185], and is likely the result of disproportionation of UO_2^+. Addition of NpO_2^+ to these samples, which is stable to disproportionation under these conditions, did not result in formation of Np(IV), suggesting that the microbes do not readily reduce actinyl(V) [185]. The presence of naturally occurring ligands, such as citrate, can effect the outcome of bioreduction, resulting in the formation of *soluble* U(IV) complexes instead of the desired *insoluble* UO_2 [188]. Bacterial reduction of uranyl has also been investigated as a means of effecting isotope fractionation [190].

A recent DFT study on the enzymatic reduction of UO_2^{2+} by *G. sulfurreducens* is consistent with the mechanism proposed above [189]. In the computational study, the reaction pathway involves the preliminary reduction of a uranyl cation to U(V). This is complexed by U(VI), resulting in a cation–cation interaction. A second reduction step gives a U(V)–U(V) dimer, which then undergoes disproportionation. During this process one of the uranyl ions is ligated by an amino acid side chain of the cytochrome c_7 protein, which facilitates the electron transfer.

5. Kinetic studies of the aqueous uranyl ion

As mentioned in Section 1, the kinetics of the ligand exchange in the actinides has recently been reviewed [1], and will not be covered here. A detailed monograph on the subject is also available [191]. Instead, the emphasis of this section will be the kinetics and mechanism of the oxygen exchange for the so-called "yl" oxygen atoms.

5.1. Exchange of the "yl" oxygen ligands under acidic conditions

Crandall, studying the exchange of H_2O in $UO_2Cl_2(H_2O)_3$, observed that all but two of the oxygen atoms are rapidly exchanged with the solvent, verifying the formula of uranyl as UO_2^{2+} [192]. The first quantitative measurements of the oxo ligand exchange in uranyl were performed by Taube and Gordon in 1961 [193]. They established the rate law shown in Eq. (8), where $k = 1.8 \times 10^{-5}$ M h^{-1}, which corresponds to a half-life of ca. 10^4 h. Given the inverse first order dependence on $[H^+]$, the exchange was presumed to take place via $[UO_2(OH)]^+$. This remarkably long half-life has been subsequently cited in numerous review articles as an example of the unique nature of the uranyl fragment [17,194,195]. For comparison, the half-life of oxo exchange in vanadyl, also under acidic conditions, is approx. 400 min at 0 °C [196]. However, Taube and Gordon also investigated the exchange of oxo ligands at higher pH ($[H^+] = 0.081$ M) and reported a much faster half life of 575 h (see Table 4 in Ref. [197]). The exchange of the uranyl oxo ligands has also been measured using ^{17}O NMR spectroscopy. With this technique, Rabideau determined the half-life for oxo exchange is 1.3×10^3 h, in 0.2 M perchloric acid [198], which is comparable to the value reported by Taube. These results were later verified by Suglobov and coworkers [199]. It should be noted that each of these studies was performed at pH < 1, whereas subsequent work was performed at higher pH (see below):

$$\text{rate} = \frac{k[UO_2^{2+}]}{[H^+]} \quad (8)$$

Suglobov and coworkers have also measured the oxo exchange in uranyl by IR spectroscopy [200,201]. They ascertained that at pH < 4 and $[UO_2^{2+}] < 0.03$ M oxo exchange was inverse 2nd order with respect to $[H^+]$ and 2nd order with respect to $[UO_2^{2+}]$ (Eq. (9)), and suggested that oxo exchange occurred via a uranyl-hydroxo dimer, $[(UO_2)_2(OH)_2]^{2+}$. The exchange, of course, would be promoted by the strongly σ-donating hydroxo ligands which are known to weaken the U=O bond (*vida supra*). However, at higher pH and higher uranyl concentration, the reaction order deviated from these parameters. They argued that as the concentration of other uranyl hydroxides increase (such as $[(UO_2)_2(OH)_3]^+$), oxo exchange in these species becomes important. Suglobov reports a rate constant of 2.7×10^{-8} mol L^{-1} s^{-1} for the low pH/low uranyl concentration regime. The invocation of $[(UO_2)_2(OH)_2]^{2+}$ as the crucial intermediate in oxo ligand exchange is corroborated by the study of uranyl hydrolysis, where $[(UO_2)_2(OH)_2]^{2+}$ is the dominant species present at moderate pH [34,202–205]:

$$\text{rate} = \frac{kK_{eq}[UO_2^{2+}]^2}{[H^+]^2} \quad (9)$$

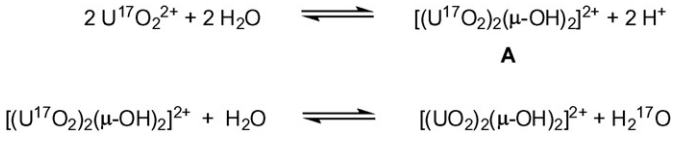

Scheme 7.

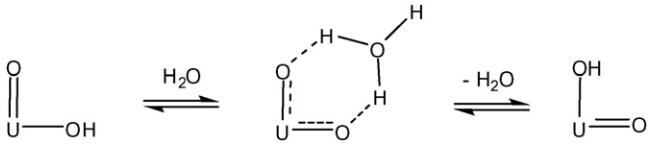

Scheme 8.

A more recent study by Grenthe and Szabó has confirmed the reaction order presented by Suglobov [206]. The Grenthe group used ^{17}O NMR spectroscopy to monitor the incorporation of labeled oxygen into uranyl. They studied the reaction between $-\log[H^+] = 1.48$ and $-\log[H^+] = 2.64$, and obtained a rate constant of $2.11 \times 10^{-2}\ h^{-1}$. They also synthesized a bridged hydroxo complex, $[UO_2(oxalate)F(\mu\text{-}OH)]_2^{4-}$, and observed no exchange of the "yl" oxygen in this species over the course of a week. From this experiment they inferred that a water molecule coordinated to the equatorial plane was required for oxo exchange. Grenthe disputes the involvement of $[(UO_2)_2(OH)_3]^+$ in the exchange mechanism, as there is little evidence that such a species exists. Instead, they propose that $[(UO_2)_3O(OH)_3]^+$, a μ_3 oxo-bridged trimer, is a likely intermediate in the higher pH regime.

The combined studies of Suglobov and Grenthe [201,206], cast some uncertainty on the original results of Taube [193]. Grenthe suggests that the complicated experimental procedure of Taube and Gordon may have introduced error into their results. However, it should be noted that the Taube experiments were performed at a significantly higher uranyl concentration [193,198], and under these conditions a different mechanistic pathway could be operative.

A mechanism consistent with the available experimental data is shown in Scheme 7 [206]. Exchange is presumed to proceed via the hydroxide bridged dimer of uranyl (**A**) [201], however a structure for the transition state which is ultimately responsible for oxo ligand exchange has not yet been proposed.

5.2. Exchange of the "yl" oxygen ligands under basic conditions

Significantly less experimental work has been performed on the exchange of the uranyl oxo ligands under basic conditions. A preliminary study, using ^{17}O NMR spectroscopy, was performed by Clark and coworkers [39]. This study used $[NEt_4][OH]$ as the hydroxide source to prevent precipitation of the normally insoluble uranyl hydroxide. Under these highly basic conditions the uranyl species present in solution was thought to be $[UO_2(OH)_5]^{3-}$. However, $[UO_2(OH)_4]^{2-}$ was the species isolated in the solid-state. It should be noted that conflicting evidence exists concerning the prevalence of $[UO_2(OH)_5]^{3-}$ and $[UO_2(OH)_4]^{2-}$ under these conditions (see below) [207,208]. The ^{17}O NMR signal for the oxo ligands in $[UO_2(OH)_5]^{3-}$ showed significant broadening upon warming, suggesting oxygen exchange with the OH^- co-ligands. A line broadening analysis provided the following activation parameters: $\Delta H^{\ddagger} = 9.8 \pm 0.3$ kcal/mol and $\Delta S^{\ddagger} = -18 \pm 4$ cal/mol K, which indicates "a thermally accessible and slightly ordered transition state" [39]. Confirmation of oxo ligand exchange was made with Raman spectroscopy, as solutions of $[UO_2(OH)_5]^{3-}$, prepared in 98% $H_2{}^{18}O$, displayed a ν_1 at 752 cm^{-1}. This is 34 cm^{-1} lower than the vibration observed using unenriched H_2O. Clark et al. speculate that the strongly donating hydroxide ligand weakens the U=O bonds (as evidenced by the low ν_1 values) making oxo exchange facile, and they propose a water assisted proton-transfer to account for the observed activation parameters (Scheme 8).

Szabó and Grenthe have recently reinvestigated the exchange of the oxo ligands in uranyl under highly alkaline conditions [206]. They followed a solution of $U^{17}O_2{}^{2+}$ in 3.5 M $[NEt_4][OH]$ by ^{17}O NMR spectroscopy and observed no change in the peak integral, suggesting that no exchange is occurring. They also suggest that the line-broadening observed by Clark et al. is not due to oxo ligand exchange but due to two-site exchange between $[UO_2(OH)_5]^{3-}$ and $[UO_2(OH)_4]^{2-}$, the two dominate uranyl species in solution. A similar conclusion was also drawn by an earlier paper [209].

As noted above, several authors doubt the prevalence of $[UO_2(OH)_5]^{3-}$ in highly alkaline environments and, based on theory and EXAFS measurements, they have suggested that $[UO_2(OH)_4]^{2-}$ predominates under these conditions [207,208,210]. In particular, the equatorial U–O bond lengths in $[UO_2(OH)_5]^{3-}$ as determined by DFT do not match the U–O(hydroxide) bond lengths for the uranyl hydroxide complex as measured by EXAFS [208,210].

The exchange of uranyl oxo ligands under basic conditions has also been investigated by DFT. In a 1998 contribution, Schreckenbach and coworkers proposed an oxo exchange mechanism for $[UO_2(OH)_4]^{2-}$ which proceeded via *cis*-uranyl intermediate **B**

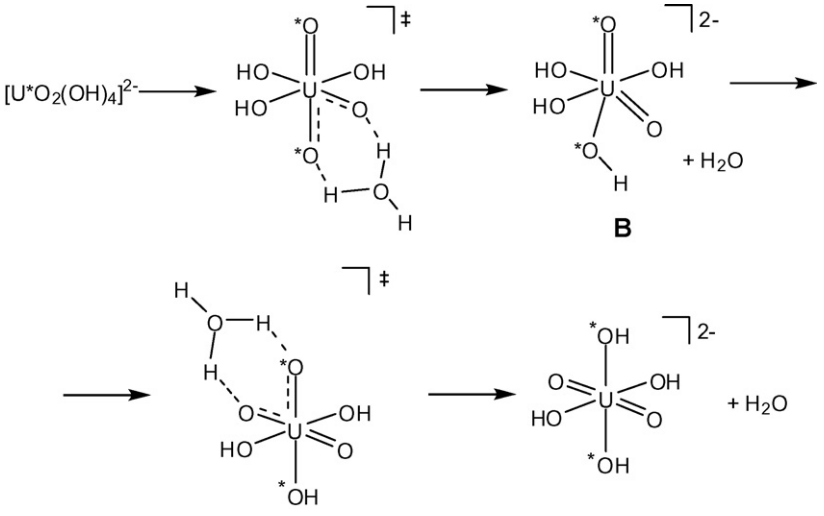

Scheme 9.

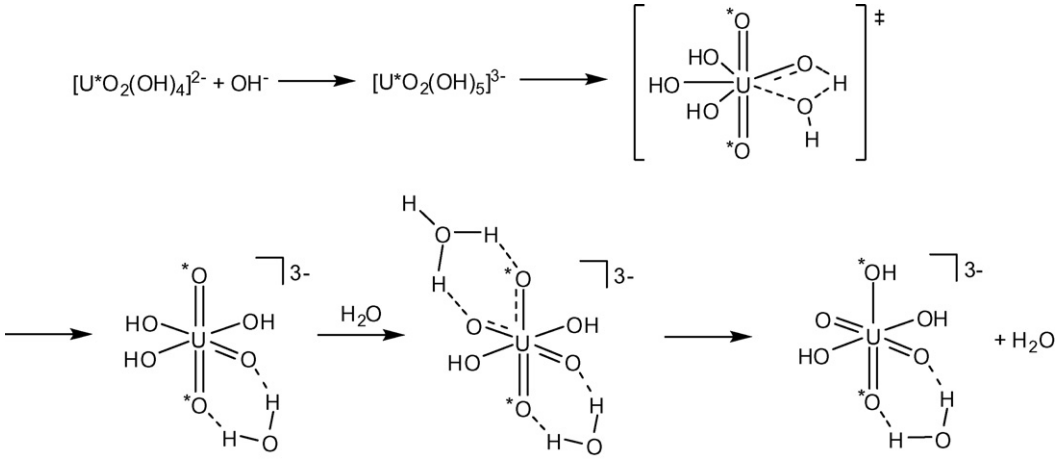

Scheme 10.

(Scheme 9) [211]. Oxo ligand exchange in $UO_2(OH)_2$ was also predicted to proceed via a *cis*-uranyl intermediate [212].

Subsequently, Schreckenbach and Shamov re-investigated the oxygen exchange in uranyl hydroxide, again using DFT, and determined that oxo exchange under highly basic conditions by a different mechanism was possible [213]. They propose a novel pathway, whereby oxo exchange occurs via a uranium trioxide intermediate, $[UO_3(OH)_3]^{3-}\cdot H_2O$ (Scheme 10). A water assisted proton shuttle was invoked to facilitate oxo ligand exchange.

Scheme 10 represents an improvement over previously suggested mechanisms, as it has the advantage of avoiding the high-energy *cis*-uranyl intermediate proposed in earlier studies [211,212,214]. Interestingly, the largest activation barrier for this process occurs upon formation of $[UO_2(OH)_5]^{3-}$ from $[UO_2(OH)_4]^{2-}$ and OH^- (and not hydroxide deprotonation).

5.3. Exchange of the "yl" oxygen ligands in neptunyl and plutonyl

Exchange of the "yl" oxygen atoms in neptunyl (NpO_2^{n+}, $n = 1$, 2) and plutonyl (PuO_2^{n+}, $n = 1$, 2) under acidic conditions has also been investigated [215–218], and the comparison of these results with those observed for uranyl is potentially insightful. Because of the paramagnetism of these actinyl ions, ^{17}O NMR spectroscopy could not be used as a monitoring technique. Instead, the actinyl ion was precipitated as its ferricyanide salt, and combusted in the presence of $HgCl_2$. The mass composition of the resulting CO_2 was then measured by mass spectrometry. This is a similar procedure to that originally used by Taube [193]. The radioactivity of Np and Pu significantly complicates measurements, as radiolysis generates the lower-valent actinide ions, which can catalyze oxo ligand exchange. As a result, experiments were performed under a Cl_2 atmosphere to quickly re-oxidize the products of radiolysis. Given these difficulties, the lower-limit for the oxo ligand exchange in PuO_2^{2+} was found to be slow, with $t_{1/2} > 10^4$ h (typical conditions: 0.15 M PuO_2^{2+}, 1.0 M $HClO_4$) [217]. This is comparable to the results observed for uranyl [193]. Further experiments determined that PuO_2^{+} was a competent catalyst for oxo ligand exchange, but Pu(III) and Pu(IV) were not [215]. From the observed acceleration of the exchange in PuO_2^{2+}, for a given amount of PuO_2^{+}, a half-life of ca. 200 h was calculated for the oxo exchange in PuO_2^{+} (conditions: 0.11 M PuO_2^{2+}, 0.0058 M PuO_2^{+}, 0.457 M $HClO_4$). Surprisingly, this is significantly longer than the half-life for oxo exchange determined for UO_2^{+}. In addition, the authors noted a pronounced acceleration of the oxo ligand exchange upon addition of 6.5 M HF to 0.11 M PuO_2^{2+} ($t_{1/2} = 17$ h). The neptunyl system (NpO_2^{n+}, $n = 1$, 2) was also investigated [216]. The half-life for the oxo ligand exchange in NpO_2^{2+} was found to be $t_{1/2} = 15$ h (typical conditions: 0.32 M NpO_2^{2+}, 1.0 M $HClO_4$). At lower acidities (0.25 M $HClO_4$) the half-life increased considerably ($t_{1/2} = 220$ h). These half-lives, however, are considerably shorter than those observed for either uranyl or plutonyl. The results for the pentavalent analog, NpO_2^{+} were qualitative, but not surprisingly they indicate that oxo ligand exchange in this species is faster than in NpO_2^{2+} [216].

5.4. Exchange of UO_2^{2+} and U(IV)

The exchange of UO_2^{2+} with U(IV) in hydrochloric acid solutions was monitored using ^{233}U as a tracer [219,220]. The exchange was found to be 2nd order with respect to U(IV), 1st order with respect to UO_2^{2+}, and inverse 3rd order with respect to H^+. Addition of chloride had no effect on the rate. Similarly, light had no effect on the reaction rate. In contrast, a subsequent study in perchloric acid found that the exchange was 1st order with respect to U(IV), 1st order with respect to UO_2^{2+}, and inverse 3rd order with respect to H^+ [221]. A rate law which accounts for this data is shown in Eq. (10) [221]. It has also been observed that addition of SO_4^{2-} increases the rate of exchange, while addition of F^- decreases the rate [222]. In the case of F^-, at least, it is likely that a uranium fluoride complex is formed which is relatively inert. The change in the reaction order with respect to U(IV) in going from HCl and $HClO_4$ is not understood, but it has been pointed out that the results in HCl were collected over a limited concentration range [220]. Subsequent work at high concentrations of HCl (<8 M) reveal an increase in the rate of exchange with increasing concentration of HCl, implying that a different mechanism is operative, probably involving the formation of a chloride complex [223]. The exchange reaction has also been studied in a mixed aqueous-organic solvent system [224–227]. As with the HCl system, the mechanism of exchange likely varies with the change in ratio of water to organic solvent [224]. The UO_2^{2+}–U(IV) exchange has also been investigated as a

$$2\,U(V) \rightleftharpoons U(VI) + U(IV)$$

$$K_{eq} = \frac{[U(IV)][U(VI)]}{[U(V)]^2}$$

Scheme 11.

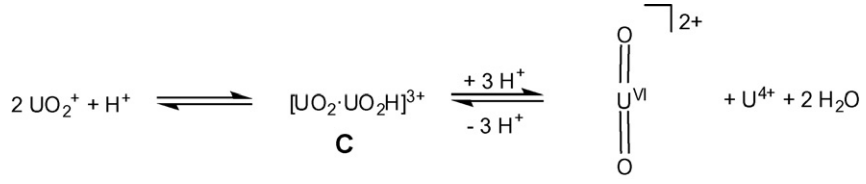

Scheme 12.

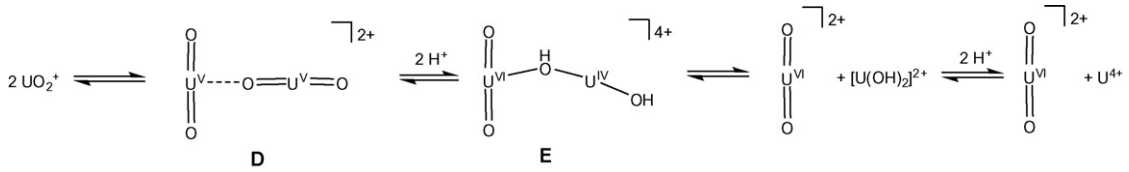

Scheme 13.

means of isotope fractionation [228].

$$\text{rate} = k\frac{[\text{U(IV)}][\text{UO}_2^{2+}]}{[\text{H}^+]^3 + \text{K}_\text{H}[\text{H}^+]^2} \quad (10)$$

where $K_\text{H} = \frac{[\text{UOH}^{3+}][\text{H}+]}{[\text{U}^{4+}]}$

The mechanism of the UO_2^{2+}–U(IV) exchange likely involves conproportionation to UO_2^+ [229,230]. The conproportionation of uranium(VI) and uranium(IV) is pH dependent, but at pH = 2–2.5, solutions which simultaneously contain UO_2^{2+}, UO_2^+, and U^{4+} can be prepared, where the dominant species present is UO_2^+ [230]. Under these conditions K_{eq} is around unity (Scheme 11) [231]. At other acidities however, the disproportionation of UO_2^+ is reported to be rapid [21,105].

The kinetics of U(V) disproportionation are well established and are 2nd order with respect to UO_2^+ and 1st order with respect to H^+ (Eq. (11)) [105,197,232–235].

$$\text{rate} = k[\text{UO}_2^+]^2[\text{H}^+] \quad (11)$$

Combining Eqs. (10) and (11) generate Scheme 12, where intermediate **C** is common to both UO_2^+ disproportionation and UO_2^{2+}–U(IV) exchange [221].

Intermediate **C** is likely a cation–cation complex, as suggested by Steele and Taylor, who have studied the disproportionation of U(V) by DFT (Scheme 13) [136]. Their cation–cation intermediate exhibits a single donor interaction, where one "yl" oxygen of a UO_2^+ ion coordinates to the equatorial plane of a second UO_2^+ ion (intermediate **D**). This arrangement is supported by several solid-state molecular structures [16,106,123], and corresponds to structure **II** as shown in Fig. 6. Protonation of the two oxo ligands of one uranyl fragment then generates a UO_2^{2+}–U(IV) complex (**E**). Electron transfer occurs after the first protonation event.

The implication of Schemes 12 and 13 is that U(IV) can also catalyze the oxo ligand exchange in UO_2^{2+}, but the experiments by Taube suggest that U(IV) is not as competent catalyst as U(V) (see below) [197]. A complicating factor in the disproportionation of UO_2^+ is its ability to form a cation–cation complex with UO_2^{2+} (which is generated by the disproportionation reaction) (Scheme 14). This dimeric species has been observed spectroscopically and was shown to slow the rate of disproportionation [105,232].

This cation-cation complex also plays an indirect role in the oxo ligand exchange of uranyl(VI). The rate of oxo ligand exchange in UO_2^+ is greater than that observed for UO_2^{2+} (by a factor of 10^7 in 0.08 M $HClO_4$) [197], making UO_2^+ a catalyst for oxo exchange in the parent ion. The rate of electron self-exchange for this complex has been calculated using Marcus theory and ranges between 1 and 15 $M^{-1}\,s^{-1}$ (Scheme 14) [236]. This closely matches the value determined by Taube in an earlier study (52 $M^{-1}\,s^{-1}$) [197]. The electron exchange in uranyl(VI)–uranyl(V) has also been studied by theoretical methods [237]. The intermediates studied included hydroxide, fluoride, or carbonate-bridged species (Scheme 15), where the hydroxide-bridged dimer exhibits the most efficient electron transfer.

The calculated rate constant for the hydroxide bridged dimer (26 $M^{-1}\,s^{-1}$) is close to the experimentally determined value. The self-exchange reaction for the neptunyl(VI)–neptunyl(V) system has also be studied by theory [238].

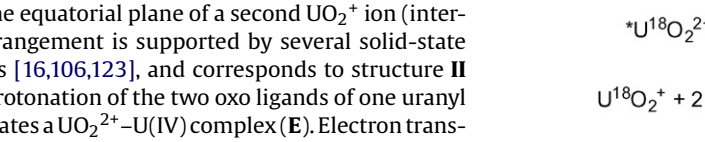

Scheme 14.

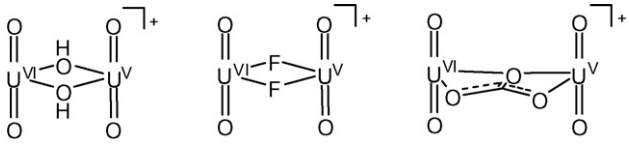

Scheme 15.

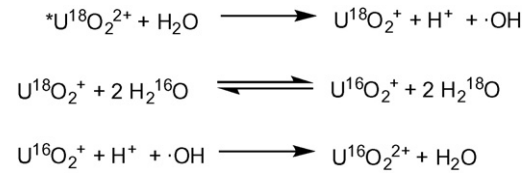

Scheme 16.

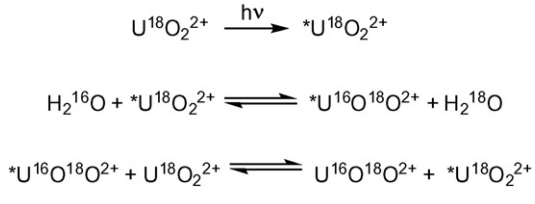

Scheme 17.

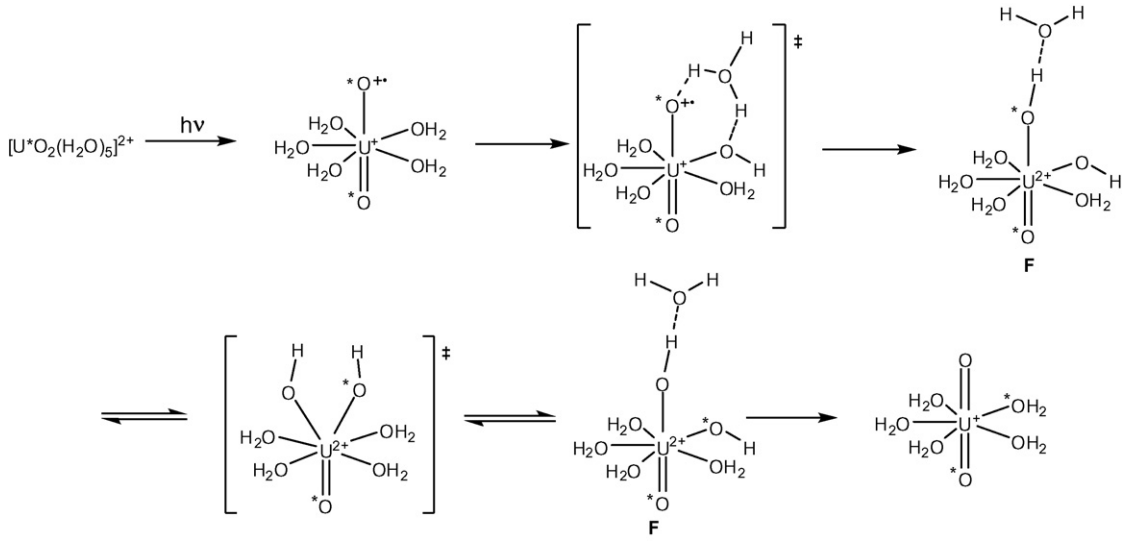

Scheme 18.

5.5. Exchange of the "yl" oxygen ligands under photolytic conditions

The exchange of the "yl" oxygen ligands in uranyl can also be photo-induced. This was first demonstrated by Taube and Gordon [197]. They assumed that photolysis was transiently generating UO_2^+, which could then catalyze oxo ligand exchange, however a subsequent theoretical study by Vallet suggests that this mechanism is unlikely [239]. The mechanism of photo-induced oxo exchange has also been studied by Suglabov and coworkers [199,240,241]. They proposed that, upon photolysis, $^*UO_2^{2+}$ oxidizes water generating UO_2^+ and ·OH. Oxo exchange then occurs in UO_2^+ before being quenched by the hydroxyl radical (Scheme 16). Interestingly, concerted exchange of both oxo ligands appears to occur at a faster rate than the exchange of a single oxo ligand [199,240,241]. Complicating the reaction scheme is the known electron exchange that occurs between UO_2^{2+} and UO_2^+ (see Section 5.4).

According to Vallet and coworkers however, the small amount of UO_2^+ present under these conditions cannot explain the extent of oxo ligand exchange [239]. With no reducing agent present, and without a substrate to oxidize, very little UO_2^+ should be formed. $^*UO_2^{2+}$ can oxidize water to form UO_2^+, but the hydroxyl radical quickly reacts with this ion, reforming UO_2^{2+} [242].

Okuyama et al. have proposed an alternate mechanism, whereby the photoexcited uranyl ion undergoes facile "yl" oxygen exchange (as opposed to the transiently generated UO_2^+ ion) [243]. The quantum yield exceeds unity, suggesting that after oxo ligand exchange the photoexcited uranyl can sensitize another uranyl ion, which can then undergo exchange itself (Scheme 17).

The mechanism of photoinduced oxo exchange has also been studied by DFT [239]. Vallet concluded that oxo ligand exchange proceeds via intramolecular proton transfer in the photoexcited uranyl ion ($^*UO_2^{2+}$). The process is facilitated by a second coordination sphere water molecule and generates a bis(hydroxo) intermediate **F** (Scheme 18). Oxo ligand exchange can then occur by facile isomerization of the two hydroxo ligands. This mechanism agrees with that proposed by Okuyama [243].

The computational study also found two excited states for the uranyl ion: a so-called "σ" state, which is characterized by equal U–O_{yl} bond lengths (both 1.76 Å) and a so-called "π" state, which is characterized by asymmetric U–O_{yl} bond lengths (1.71 and 1.94 Å). The "σ" state corresponds to the normal luminescent excited state

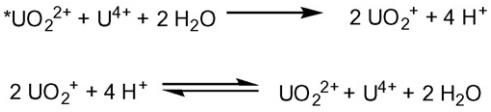

Scheme 19.

of uranyl, while the "π" state is slightly higher in energy and responsible for oxo ligand exchange. In addition, the more distant oxo ligand of this state exhibits a partial positive charge and significant radical character [239].

Photo-stimulated oxo exchange has been qualitatively studied using ^{17}O NMR spectroscopy [244] and IR spectroscopy [200]. In addition, exchange of U(VI) with U(IV) was also found to be photo-accelerated [245]. The mechanism probably involves oxidation of U^{4+} by $^*UO_2^{2+}$ generating 2 equiv. of UO_2^+ (Scheme 19). UO_2^+ can then disproportionate via its usual mechanism [105].

6. Summary

In recent years we have witnessed a renaissance of uranyl chemistry. Significant advancements include the synthesis of the imido analogs of uranyl [246,247], the synthesis and structural characterization of many new pentavalent uranyl complexes [13,16,31,104,248], and the controlled silylation of the uranyl oxo ligands [45]. Eventually, these discoveries may lead to improvements in nuclear fuel processing (of which uranyl is a major component) and new methods for decontamination at legacy sites. The uranyl ion has long been regarded as a unique molecular fragment. The experiments described in this review have not changed this assessment, but they have served to lift some of the mystery surrounding this species, allowing us to better understand how its unique properties arise.

References

[1] Z. Szabo, T. Toraishi, V. Vallet, I. Grenthe, Coord. Chem. Rev. 250 (2006) 784–815.
[2] C.R. Graves, J.L. Kiplinger, Chem. Commun. (2009) 3831–3853.
[3] P.L. Arnold, J.B. Love, D. Patel, Coord. Chem. Rev 253 (2009) 1973–1978.
[4] J.D. Van Horn, H. Huang, Coord. Chem. Rev. 250 (2006) 765–775.
[5] J.L. Sessler, P.J. Melfi, D.G. Pantos, Coord. Chem. Rev. 250 (2006) 816–843.
[6] R.G. Denning, J. Phys. Chem. A 111 (2007) 4125–4143.
[7] N.W. Alcock, D.J. Flanders, D. Brown, Dalton Trans. (1984) 679–681.

[8] J. Maynadie, J.-C. Berthet, P. Thuery, M. Ephritikhine, Chem. Commun. (2007) 486–488.
[9] M.P. Wilkerson, C.J. Burns, D.E. Morris, R.T. Paine, B.L. Scott, Inorg. Chem. 41 (2002) 3110–3120.
[10] M.J. Sarsfield, M. Helliwell, J. Raftery, Inorg. Chem. 43 (2004) 3170–3179.
[11] J.-C. Berthet, M. Nierlich, M. Ephritikhine, Dalton Trans. (2004) 2814–2821.
[12] J.-C. Berthet, M. Nierlich, M. Ephritikhine, Chem. Commun. (2003) 1660–1661.
[13] L. Natrajan, F. Burdet, J. Pécaut, M. Mazzanti, J. Am. Chem. Soc. 128 (2006) 7152–7153.
[14] J.-C. Berthet, G. Siffredi, P. Thuéry, M. Ephritikhine, Chem. Commun. (2006) 3184–3186.
[15] J.-C. Berthet, M. Nierlich, M. Ephritikhine, Angew. Chem., Int. Ed. 42 (2003) 1952–1954.
[16] F. Burdet, J. Pecaut, M. Mazzanti, J. Am. Chem. Soc. 128 (2006) 16512–16513.
[17] R.G. Denning, Struct. Bonding 79 (1992) 215–276.
[18] S. Cotton, Lanthanide and Actinide Chemistry, John Wiley & Sons Ltd., West Sussex, England, 2006.
[19] A. Fischer, Z. Anorg, Allg. Chem. 629 (2003) 1012–1016.
[20] L.R. Morss, N.M. Edelstein, J. Fuger, J.J. Katz (Eds.), The Chemistry of the Actinide and Transactinide Elements, Springer, 2006.
[21] J. Selbin, J.D. Ortego, Chem. Rev. 69 (1969) 657–671.
[22] I. Grenthe, J. Fuger, R.J.M. Konings, R.J. Lemire, A.B. Muller, C. Nguyen-Tsung Cregu, H. Wanner, Chemical Thermodynamics of Uranium, Elsevier, New York, 1992.
[23] D.E. Morris, Inorg. Chem. 41 (2002) 3542–3547.
[24] J.M. Winfield, G.M. Andersen, J. Iqbal, D.W.A. Sharp, J.H. Cameron, A.G. McLeod, J. Fluor. Chem. 24 (1984) 303–317.
[25] S. Fortier, G. Wu, T.W. Hayton, Inorg. Chem. 47 (2008) 4752–4761.
[26] E. Bosse, C. Den Auwer, C. Berthon, P. Guilbaud, M.S. Grigoriev, S. Nikitenko, C.L. Naour, C.l. Cannes, P. Moisy, Inorg. Chem. 47 (2008) 5746–5755.
[27] S.I. Nikitenko, C. Cannes, C. Le Naour, P. Moisy, D. Trubert, Inorg. Chem. 44 (2005) 9497–9505.
[28] C.J. Burns, W.H. Smith, J.C. Huffman, A.P. Sattelberger, J. Am. Chem. Soc. 112 (1990) 3237–3239.
[29] S. Fortier, G. Wu, T.W. Hayton, Inorg. Chem. 48 (2009) 3000–3011.
[30] C.C. Cummins, K. Meyer, D.J. Mindiola, T.A. Baker, W.M. Davis, Angew. Chem. Int. Ed. 39 (2000) 3063–3066.
[31] T.W. Hayton, G. Wu, Inorg. Chem. 47 (2008) 7415–7423.
[32] K. Mizuoka, S. Tsushima, M. Hasegawa, T. Hoshi, Y. Ikeda, Inorg. Chem. 44 (2005) 6211–6218.
[33] G. Gritzner, J. Selbin, J. Inorg. Nucl. Chem. 30 (1968) 1799–1804.
[34] F. Quilès, A. Burneau, Vib. Spectrosc. 23 (2000) 231–241.
[35] C. Nguyen Trung, G.M. Begun, D.A. Palmer, Inorg. Chem. 31 (1992) 5280–5287.
[36] S.P. McGlynn, J.K. Smith, W.C. Neely, J. Chem. Phys. 35 (1961) 105–116.
[37] L.M. Toth, G.M. Begun, J. Phys. Chem. 85 (1981) 547–549.
[38] M.J. Sarsfield, M. Helliwell, J. Am. Chem. Soc. 126 (2004) 1036–1037.
[39] D.L. Clark, S.D. Conradson, R.J. Donohoe, D.W. Keogh, D.E. Morris, P.D. Palmer, R.D. Rogers, C.D. Tait, Inorg. Chem. 38 (1999) 1456–1466.
[40] P. Arnold, D. Patel, A.J. Blake, C. Wilson, J.B. Love, J. Am. Chem. Soc. 128 (2006) 9610–19610.
[41] P.G. Allen, J.J. Bucher, D.L. Clark, N.M. Edelstein, S.A. Ekberg, J.W. Gohdes, E.A. Hudson, N. Kaltsoyannis, W.W. Lukens, M.P. Neu, P.D. Palmer, T. Reich, D.K. Shuh, C.D. Tait, B.D. Zwick, Inorg. Chem. 34 (1995) 4797–4807.
[42] K.I.M. Ingram, L.J.L. Haller, N. Kaltsoyannis, Dalton Trans. (2006) 2403–2414.
[43] M.P. Wilkerson, C.J. Burns, H.J. Dewey, J.M. Martin, D.E. Morris, R.T. Paine, B.L. Scott, Inorg. Chem. 39 (2000) 52577–55285.
[44] C.J. Burns, D.L. Clark, R.J. Donohoe, P.B. Duval, B.L. Scott, C.D. Tait, Inorg. Chem. 39 (2000) 5464–5468.
[45] P. Arnold, D. Patel, C. Wilson, J.B. Love, Nature 451 (2008) 315–318.
[46] J.R. Galsworthy, M.L.H. Green, M. Müller, K. Prout, Dalton Trans. (1997) 1309–1314.
[47] L.H. Doerrer, J.R. Galsworthy, M.L.H. Green, M.A. Leech, Dalton Trans. (1998) 2483–2488.
[48] L.H. Doerrer, J.R. Galsworthy, M.L.H. Green, M.A. Leech, M. Müller, Dalton Trans. (1998) 3191–3194.
[49] T.W. Hayton, G. Wu, Inorg. Chem. 48 (2009) 3065–3072.
[50] J.J. Berard, G. Schreckenbach, P. Arnold, D. Patel, J.B. Love, Inorg. Chem. 47 (2008) 11583–11592.
[51] D.M. Barnhart, C.J. Burns, N.N. Sauer, J.G. Watkin, Inorg. Chem. 34 (1995) 4079–4084.
[52] P. Thuery, B. Masci, M. Takimoto, T. Yamato, Inorg. Chem. Commun. 10 (2007) 795–799.
[53] P. Thuéry, B. Masci, Dalton Trans. (2003) 2411–2417.
[54] P. Thuéry, B. Masci, Polyhedron 23 (2004) 649–654.
[55] B. Masci, P. Thuéry, CrystEngComm 9 (2007) 582–590.
[56] P. Thuéry, Polyhedron 26 (2007) 101–106.
[57] P.A. Giesting, N.J. Porter, P.C. Burns, Z. Kristallogr. 221 (2006) 589–599.
[58] P. Thuéry, Chem. Commun. (2006) 853–855.
[59] M. Cametti, M. Nissinen, A. Dalla Cort, L. Mandolini, K. Rissanen, J. Am. Chem. Soc. 127 (2005) 3831–3837.
[60] M. Cametti, M. Nissinen, A. Dalla Cort, K. Rissanen, L. Mandolini, Inorg. Chem. 45 (2006) 6099–6101.
[61] J.A. Danis, M.R. Lin, B.L. Scott, B.W. Eichhorn, W. Runde, Inorg. Chem. 40 (2001) 3389–3394.
[62] M.-J. Crawford, P. Mayer, Inorg. Chem. 44 (2005) 8481–8485.
[63] P. Finch, P.C. Burns (Eds.), Uranium: Mineralogy, Geochemistry and the Environment, Mineralogical Society of America, Washington, D.C, 1999.
[64] P.D. Wilson (Ed.), The Nuclear Fuel Cycle: From Ore to Wastes, Oxford University Press, Oxford, 1996.
[65] P.C. Burns, Can. Miner. 43 (2005) 1839–1894.
[66] E. Gebert, H.R. Hoekstra, A.H. Reis Jr., S.W. Peterson, J. Inorg. Nucl. Chem. 40 (1978) 65–68.
[67] E.H.P. Cordfunke, D.J.W. Ijdo, J. Solid State Chem. 115 (1995) 299–304.
[68] J. Jove, A. Cousson, M. Gasperin, J. Less-Common Met. 139 (1988) 345–350.
[69] W.H. Zachariasen, Acta Cryst. 7 (1954) 788–791.
[70] W.H. Zachariasen, Acta Cryst. 1 (1948) 281–285.
[71] A.H. Reis Jr., H.R. Hoekstra, E. Gebert, S.W. Peterson, J. Inorg. Nucl. Chem. 38 (1976) 1481–1485.
[72] W. Zhang, J. Zhao, Inorg. Chem. Commun. 9 (2006) 397–399.
[73] W. Zhang, J. Zhao, J. Mol. Struct. 789 (2006) 177–181.
[74] A. Coda, A.D. Giusta, V. Tazzoli, Acta Cryst. B 37 (1981) 1496–1500.
[75] P.M. Almond, T.E. Albrecht-Schmitt, Inorg. Chem. 41 (2002) 5495–5501.
[76] A.C. Bean, Y. Xu, J.A. Danis, T.E. Albrecht-Schmitt, B.L. Scott, W. Runde, Inorg. Chem. 41 (2002) 6775–6779.
[77] M.K. Pagoaga, D.E. Appleman, J.M. Stewart, Am. Miner. 72 (1987) 1230–1238.
[78] F. Demartin, V. Diella, S. Donzelli, C.M. Gramaccioli, T. Pilati, Acta Cryst. B 47 (1991) 439–446.
[79] S.V. Krivovichev, P.C. Burns, Inorg. Chem. 41 (2002) 4108–4110.
[80] U. Kolitsch, G. Giester, Miner. Mag. 65 (2001) 717–724.
[81] A.J. Locock, P.C. Burns, Can. Miner. 41 (2003) 489–502.
[82] C.L. Cahill, D.T. de Lill, M. Frisch, CrystEngComm 9 (2007) 15–26.
[83] W. Chen, H.-M. Yuan, J.-Y. Wang, Z.-Y. Liu, J.-J. Xu, M. Yang, J.-S. Chen, J. Am. Chem. Soc. 125 (2003) 9266–9267.
[84] T.Y. Shvareva, T.E. Albrecht-Schmitt, Inorg. Chem. 45 (2006) 1900–1902.
[85] T.L. Cremers, P.G. Eller, E.M. Larson, Acta Cryst. C 42 (1986) 1684–1685.
[86] J.C. Taylor, P.W. Wilson, Acta Cryst. B 30 (1974) 169–175.
[87] R.D. Rogers, A.H. Bond, W.G. Hipple, A.N. Rollins, R.F. Henry, Inorg. Chem. 30 (1991) 2671–2679.
[88] T.S. Franczyk, K.R. Czerwinski, K.N. Raymond, J. Am. Chem. Soc. 114 (1992) 8138–8146.
[89] P.H. Walton, K.N. Raymond, Inorg. Chim. Acta 240 (1995) 593–601.
[90] B. Masci, M. Gabrielli, S.L. Mortera, M. Nierlich, P. Thuery, Polyhedron 21 (2002) 1125–1131.
[91] P.L. Arnold, A.J. Blake, C. Wilson, J.B. Love, Inorg. Chem. 43 (2004) 8206–8208.
[92] M.-L. Tong, X.-M. Chen, Y.-Z. Zheng, Eur. J. Inorg. Chem. (2005) 4109–4117.
[93] P. Thuéry, M. Nierlich, Dalton Trans. (1997) 1481–1482.
[94] P.S. Halasyamani, R.J. Francis, S.M. Walker, D. O'Hare, Inorg. Chem. 38 (1999) 271–279.
[95] S.V. Krivovichev, P.C. Burns, J. Solid State Chem. 170 (2003) 106–117.
[96] J.-Y. Kim, A.J. Norquist, D. O'Hare, Dalton Trans. (2003) 2813–2814.
[97] K.M. Ok, J. Baek, P.S. Halasyamani, D. O'Hare, Inorg. Chem. 45 (2006) 10207–10214.
[98] V. Vallet, T. Privalov, U. Wahlgren, I. Grenthe, J. Am. Chem. Soc. 126 (2004) 7766–7767.
[99] D. Hagberg, G. Karlstrom, B.O. Roos, L. Gagliardi, J. Am. Chem. Soc. 127 (2005) 14250–14256.
[100] P. Nichols, E.J. Bylaska, G.K. Schenter, W. de Jong, J. Chem. Phys. 128 (2008) 124507.
[101] P. Guilbaud, G. Wipff, J. Phys. Chem. 97 (1993) 5685–5692.
[102] S. Tsushima, Inorg. Chem 48 (2009) 4856–4862.
[103] L. Shapiro, A.M. Fannon, P.D. Kwong, A. Thompson, M.S. Lehmann, G. Grubel, J.-F. Legrand, J. Als-Nielson, D.R. Colman, W.A. Hendrickson, Nature 374 (1995) 327–337.
[104] G. Nocton, P. Horeglad, J. Pecaut, M. Mazzanti, J. Am. Chem. Soc. 130 (2008) 16633–16645.
[105] A. Ekstrom, Inorg. Chem. 13 (1974) 2237–2241.
[106] N.N. Krot, M.S. Grigoriev, Russ. Chem. Rev. 73 (2004) 89–100.
[107] A. Cousson, S. Dabos, H. Abazli, F. Nectoux, M. Pagès, G. Choppin, J. Less Common Met. 99 (1984) 233–240.
[108] M.S. Grigoriev, N.N. Krot, A.A. Bessonov, K.Y. Suponitsky, Acta Cryst. Sect. E E63 (2007) m561–m562.
[109] T.E. Albrecht-Schmitt, P.M. Almond, R.E. Sykora, Inorg. Chem. 42 (2003) 3788–3795.
[110] B. Guillaume, R.L. Hahn, A.H. Narten, Inorg. Chem. 22 (1983) 109–111.
[111] B. Guillaume, G.M. Begun, R.L. Hahn, Inorg. Chem. 21 (1982) 1159–1166.
[112] N.J. Stoyer, D.C. Hoffman, R.J. Silva, Radiochim. Acta 88 (2000) 279.
[113] I.A. Charushnikova, N.N. Krot, Z.A. Starikova, Radiochim. Acta 95 (2007) 495–499.
[114] B. Guillaume, D.E. Hobart, J.Y. Bourges, J. Inorg. Nucl. Chem. 43 (1981) 3295–3299.
[115] T.Z. Forbes, P.C. Burns, L. Soderholm, S. Skanthakumar, Chem. Mater. 18 (2006) 1643–1649.
[116] S. Siegel, H.R. Hoekstra, E. Sherry, Acta Cryst. 20 (1966) 292–295.
[117] N.P. Brandenburg, B.O. Loopstra, Acta Cryst. B 34 (1978) 3734–3736.
[118] V.N. Serezhkin, N.V. Boiko, L.G. Makarevich, Kristallografiya 25 (1980) 858–860.
[119] J.C. Taylor, P.W. Wilson, Acta Cryst. B 29 (1973) 1073–1076.
[120] S. Siegel, A. Viste, H.R. Hoekstra, B. Tani, Acta Cryst. B 28 (1972) 117–121.
[121] J.C. Taylor, A. Ekstrom, C.H. Randall, Inorg. Chem. 17 (1978) 3285–3289.
[122] D. Rose, Y.-D. Chang, Q. Chen, J. Zubieta, Inorg. Chem. 33 (1994) 5167–5168.

[123] T.A. Sullens, R.A. Jensen, T.Y. Shvareva, T.E. Albrecht-Schmitt, J. Am. Chem. Soc. 126 (2004) 2676–2677.
[124] P. Thuery, M. Nierlich, B. Souley, Z. Asfari, J. Vicens, Dalton Trans. (1999) 2589–2594.
[125] Y. Li, C.L. Cahill, P.C. Burns, Chem. Mater. 13 (2001) 4026–4031.
[126] K.-A. Kubatko, P.C. Burns, Inorg. Chem. 45 (2006) 10277–10281.
[127] E.V. Alekseev, S.V. Krivovichev, T. Malcherek, W. Depmeier, Inorg. Chem. 46 (2007) 8442–8444.
[128] S. Obbade, S. Yagoubi, C. Dion, M. Saadi, F. Abraham, J. Solid State Chem. 177 (2004) 1681–1694.
[129] E.V. Alekseev, S.V. Krivovichev, W. Depmeier, O.I. Siidra, K. Knorr, E.V. Suleimanov, E.V. Chuprunov, Angew. Chem., Int. Ed. 45 (2006) 7233–7235.
[130] S.V. Krivovichev, Radiokhimiya 50 (2008) 389–392.
[131] S. Obbade, C. Dion, M. Rivenet, M. Saadi, F. Abraham, J. Solid State Chem. 177 (2004) 2058–2067.
[132] A.M. Chippindale, P.G. Dickens, G.J. Flynn, G.P. Stuttard, J. Mater. Chem. 5 (1995) 141–146.
[133] R. Cea-Olivares, G. Canseco-Melchor, M.M. Moya-Cabrera, V. Garcia-Montalvo, J.G. Alvarado-Rodriguez, R.A. Toscano, Inorg. Chem. Commun. 8 (2005) 205–207.
[134] M.L. McKee, M. Swart, Inorg. Chem. 44 (2005) 6975–6982.
[135] A. Ekstrom, H. Loeh, C.H. Randall, L.L. Szego, J.C. Taylor, Inorg. Nucl. Chem. Lett. 14 (1978) 301–304.
[136] H. Steele, R.J. Taylor, Inorg. Chem. 46 (2007) 6311–6318.
[137] R. Hille, Chem. Rev. 96 (1996) 2757–2816.
[138] L.M. Thomson, M.B. Hall, J. Am. Chem. Soc. 123 (2001) 3995–4002.
[139] A.L. Odom, D.J. Mindiola, C. Cummins, Inorg. Chem. 38 (1999) 3290–3295.
[140] C.-M. Che, J.-L. Zhang, R. Zhang, J.-S. Huang, T.-S. Lai, W.-M. Tsui, X.-G. Zhou, Z.-Y. Zhou, N. Zhu, C.K. Chang, Chem. Eur. J. 11 (2005) 7040–7053.
[141] J.J. Kennedy-Smith, K.A. Nolin, H.P. Gunterman, F.D. Toste, J. Am. Chem. Soc. 125 (2003) 4056–4057.
[142] H. Li, P. Palanca, V. Sanz, M.T. Picher, L.R. Domingo, A. Domenech, J.-V. Folgado, Inorg. Chim. Acta 268 (1998) 145–150.
[143] N. Jin, M. Ibrahim, T.G. Spiro, J.T. Groves, J. Am. Chem. Soc. 129 (2007) 12416–12417.
[144] D.C. Bradley, R.C. Mehrotra, I.P. Rothwell, A. Singh, Alkoxo and Aryloxo Derivatives of Metals, Academic Press, San Diego, 2001.
[145] D.C. Bradley, A.K. Chatterjee, A.K. Chatterjee, J. Inorg. Nucl. Chem. 12 (1959) 71–78.
[146] C.J. Burns, A.P. Sattelberger, Inorg. Chem. 27 (1988) 3692–3693.
[147] P.C. Leverd, D. Rinaldo, M. Nierlich, Dalton Trans. (2002) 829–831.
[148] P.C. Leverd, P. Berthault, M. Lance, M. Nierlich, Eur. J. Inorg. Chem. (1998) 1859–1862.
[149] P.B. Duval, C.J. Burns, W.E. Buschmann, D.L. Clark, D.E. Morris, B.L. Scott, Inorg. Chem. 40 (2001) 5491–5496.
[150] K.W. Bagnall, J.G.H. du Preez, Chem. Commun. (1973) 820–821.
[151] K.W. Bagnall, J.G.H. du Preez, B.J. Gellatly, J.H. Holloway, Dalton Trans. (1975) 1963–1968.
[152] J.F. de Wet, J.G.H. Du Preez, Dalton Trans. (1978) 592–597.
[153] J.-C. Berthet, G. Siffredi, P. Thuery, M. Ephritikhine, Eur. J. Inorg. Chem. (2007) 4017–4020.
[154] J.-C. Berthet, P. Thuery, M. Ephritikhine, Chem. Commun. (2005) 3415–3417.
[155] C.P. Baird, T.J. Kemp, Prog. React. Kinet. 22 (1997) 87–139.
[156] V. Balzani, F. Bolletta, M.T. Gandolfi, M. Maestri, Top. Curr. Chem. 75 (1978) 1–64.
[157] R. Nagaishi, Y. Katsumura, K. Ishigure, H. Aoyagi, Z. Yoshida, T. Kimura, Y. Kato, J. Photochem. Photobiol. A 146 (2002) 157–161.
[158] W.D. Wang, A. Bakac, J.H. Espenson, Inorg. Chem. 34 (1995) 6034–6039.
[159] W.L. Waltz, J. Lilie, X. Xu, P. Sedlák, H. Möckel, Inorg. Chim. Acta 285 (1999) 322–325.
[160] Y. Mao, A. Bakac, Inorg. Chem. 35 (1996) 3925–3930.
[161] T.M. McCleskey, C.J. Burns, W. Tumas, Inorg. Chem. 38 (1999) 5924–5925.
[162] T.M. McCleskey, T.M. Foreman, E.E. Hallman, C.J. Burns, N.N. Sauer, Environ. Sci. Technol. 35 (2001) 547–551.
[163] G.S. Forbes, L.J. Heidt, J. Am. Chem. Soc. 56 (1934) 2363–2365.
[164] S. Kannan, A.E. Vaughn, E.M. Weis, C.L. Barnes, P.B. Duval, J. Am. Chem. Soc. 128 (2006) 14024–14025.
[165] S. Kannan, M.A. Moody, C.L. Barnes, P.B. Duval, Inorg. Chem. 45 (2006) 9206–9212.
[166] G.H. John, I. May, C.A. Sharrad, A.D. Sutton, D. Collision, M. Helliwell, M.J. Sarsfield, Inorg. Chem. 44 (2005) 7606–7615.
[167] H. Greiwing, B. Krebs, A.A. Pinkerton, Inorg. Chim. Acta 234 (1995) 127–130.
[168] R.J. Francis, P.S. Halasyamani, D. O'Hare, Chem. Mater. 10 (1998) 3131–3133.
[169] R.J. Francis, P.S. Halasyamani, D. O'Hare, Angew. Chem., Int. Ed. 37 (1998) 2214–2217.
[170] R.J. Francis, P.S. Halasyamani, J.S. Bee, D. O'Hare, J. Am. Chem. Soc. 121 (1999) 1609–1610.
[171] S.M. Walker, P.S. Halasyamani, S. Allen, D. O'Hare, J. Am. Chem. Soc. 121 (1999) 10513–10521.
[172] P.M. Almond, L. Deakin, M.J. Porter, A. Mar, T.E. Albrecht-Schmitt, Chem. Mater. 12 (2000) 3208–3213.
[173] P.M. Almond, L. Deakin, A. Mar, T.E. Albrecht-Schmitt, J. Solid State Chem. 158 (2001) 87–93.
[174] P.M. Almond, L. Deakin, A. Mar, T.E. Albrecht-Schmitt, Inorg. Chem. 40 (2001) 886–890.
[175] C.L. Cahill, P.C. Burns, Inorg. Chem. 40 (2001) 1347–1351.
[176] C.-S. Chen, S.-F. Lee, K.-H. Lii, J. Am. Chem. Soc. 127 (2005) 12208–12209.
[177] C.-H. Lin, C.-S. Chen, A.A. Shiryaev, Y.V. Zubavichus, K.-H. Lii, Inorg. Chem. 47 (2008) 4445–4447.
[178] N. Belai, M. Frisch, E.S. Ilton, B. Ravel, C.L. Cahill, Inorg. Chem. 47 (2008) 10135–10140.
[179] A.C. Bean, T.A. Sullens, W. Runde, T.E. Albrecht-Schmitt, Inorg. Chem. 42 (2003) 2628–2633.
[180] C.E. Talley, A.C. Bean, T.E. Albrecht-Schmitt, Inorg. Chem. 39 (2000) 5174–5175.
[181] D.R. Lovely, Science 293 (2001) 1444–1446.
[182] W.-M. Wu, J. Carley, M. Fienen, T. Mehlhorn, K. Lowe, J. Nyman, J. Luo, M.E. Gentile, R. Rajan, D. Wagner, R.F. Hickey, B. Gu, D. Watson, O.A. Cirpka, P.K. Kitanidis, P.M. Jardine, C.S. Criddle, Environ. Sci. Technol. 40 (2006) 3978–3985.
[183] A. Abdelouas, W. Lutze, H.E. Nuttall, in: P. Finch, P.C. Burns (Eds.), Uranium: Mineralogy, Geochemistry and the Environment, Mineralogical Society of America, Washington, D.C, 1999.
[184] D.R. Lovely, E.J.P. Phillips, Y.A. Gorby, E.R. Landa, Nature 350 (1991) 413–416.
[185] J.C. Renshaw, L.J.C. Butchins, F.R. Livens, I. May, J.M. Charnock, J.R. Lloyd, Environ. Sci. Technol. 39 (2005) 5657–5660.
[186] R.T. Anderson, H.A. Vrionis, I. Ortiz-Bernad, C.T. Resch, P.E. Long, R. Dayvault, K. Karp, S. Marutzky, D.R. Metzler, A. Peacock, D.C. White, M. Lowe, D.R. Lovely, Appl. Environ. Microbiol. 69 (2003) 5884–5891.
[187] W.-M. Wu, J. Carley, T. Gentry, M.A. Ginder-Vogel, M. Fienen, T. Mehlhorn, H. Yan, S. Caroll, M.N. Pace, J. Nyman, J. Luo, M.E. Gentile, M.W. Fields, R.F. Hickey, B. Gu, D. Watson, O.A. Cirpka, J. Zhou, S. Fendorf, P.K. Kitanidis, P.M. Jardine, C.S. Criddle, Environ. Sci. Technol. 40 (2006) 3986–3995.
[188] A.J. Francis, C.J. Dodge, Environ. Sci. Technol. 42 (2008) 8277–8282.
[189] M. Sundararajan, A.J. Campbelll, I.H. Hillier, J. Phys. Chem. A 112 (2008) 4451–4457.
[190] L.K. Rademacher, C.C. Lundstrom, T.M. Johnson, R.A. Sanford, J. Zhao, Z. Zhang, Environ. Sci. Technol. 40 (2006) 6943–6948.
[191] T.W. Newton, The Kinetics of the Reduction-Oxidation Reactions of Uranium, Neptunium, Plutonium, and Americium in Aqueous Solutions, US Energy and Development Administration, Oak Ridge, TN, 1975.
[192] H.W. Crandall, J. Chem. Phys. 17 (1949) 602–606.
[193] G. Gordon, H. Taube, J. Inorg. Nucl. Chem. 16 (1961) 189–191.
[194] C.K. Jørgensen, R. Reisfeld, J. Electrochem. Soc. 130 (1983) 681–684.
[195] C.K. Jørgensen, R. Reisfeld, Struct. Bonding 50 (1982) 121–172.
[196] M.D. Johnson, R.K. Murmann, Inorg. Chem. 22 (1983) 1068–1072.
[197] G. Gordon, H. Taube, J. Inorg. Nucl. Chem. 16 (1961) 272–278.
[198] S.W. Rabideau, J. Phys. Chem. 71 (1967) 2747.
[199] S.A. Gaziev, N.G. Gorshkov, L.G. Mashirov, D.N. Suglobov, Inorg. Chim. Acta 139 (1987) 345–351.
[200] S.A. Gaziev, N.A. Gorshkov, L.G. Mashirov, D.N. Suglobov, Radiokhimiya 26 (1984) 316–322.
[201] L.G. Mashirov, V.A. Mikhalev, D.N. Suglobov, C.R. Chimie 7 (2004) 1179–1184.
[202] D.L. Cole, E.M. Eyring, D.T. Rampton, A. Silzars, R.P. Jensen, J. Phys. Chem. 71 (1967) 2771–2775.
[203] K. Müller, V. Brendler, H. Foerstendorf, Inorg. Chem. 47 (2008) 10127–10134.
[204] R.M. Rush, J.S. Johnson, J. Phys. Chem. 67 (1963) 821–825.
[205] R.M. Rush, J.S. Johnson, K.A. Kraus, Inorg. Chem. 1 (1962) 378–386.
[206] Z. Szabo, I. Grenthe, Inorg. Chem. 46 (2007) 9372–9378.
[207] K.I.M. Ingram, J.L. Häller, N. Kaltsoyannis, Dalton Trans. (2006) 2403–2414.
[208] U. Wahlgren, H. Moll, I. Grenthe, B. Schimmelpfennig, L. Maron, V. Vallet, O. Gropen, J. Phys. Chem. A 103 (1999) 8257–8264.
[209] H. Moll, T. Reich, Z. Szabo, Radiochim. Acta 88 (2000) 411–415.
[210] V. Vallet, U. Wahlgren, B. Schimmelpfennig, H. Moll, Z. Szabo, I. Grenthe, Inorg. Chem. 40 (2001) 3516–3525.
[211] G. Schreckenbach, P.J. Hay, R.L. Martin, Inorg. Chem. 37 (1998) 4442–4451.
[212] H.P. Hratchian, J.L. Sonnenberg, P.J. Hay, R.L. Martin, B.E. Bursten, H.B. Schlegel, J. Phys. Chem. A 109 (2005) 8579–8586.
[213] G.A. Shamov, G. Schreckenbach, J. Am. Chem. Soc. 130 (2008) 13735–13744.
[214] G. Schreckenbach, P.J. Hay, R.L. Martin, J. Comput. Chem. 20 (1999) 70–90.
[215] S.W. Rabideau, B.J. Masters, J. Phys. Chem. 67 (1963) 318–323.
[216] S.W. Rabideau, J. Phys. Chem. 67 (1963) 2655–2659.
[217] B.J. Masters, S.W. Rabideau, Inorg. Chem. 2 (1963) 1–5.
[218] W.L. Reynolds, R.W. Lumry, Mechanisms of Electron Transfer, Ronald Press, New York, 1966.
[219] E. Rona, J. Am. Chem. Soc. 72 (1950) 4339–4343.
[220] T.W. Newton, S.W. Rabideau, J. Phys. Chem. 63 (1959) 365–370.
[221] B.J. Masters, L.L. Schwartz, J. Am. Chem. Soc. 83 (1961) 2620–2624.
[222] A. Ekstrom, G.E. Batley, T.M. Florence, Y.J. Farrar, J. Inorg. Nucl. Chem. 36 (1974) 2355–2359.
[223] H. Tomiyasu, H. Fukutomi, H. Kakihana, J. Inorg. Nucl. Chem. 30 (1968) 2501–2511.
[224] J.O. Wear, J. Inorg. Nucl. Chem. 25 (1963) 1445–1455.
[225] S.L. Melton, A. Indelli, E.S. Amis, J. Inorg. Nucl. Chem. 17 (1961) 325–333.
[226] D.M. Mathews, J.D. Hefley, E.S. Amis, J. Phys. Chem. 63 (1959) 1236–1240.
[227] A. Indelli, E.S. Amis, J. Am. Chem. Soc. 81 (1959) 4180–4182.
[228] T.M. Florence, G.E. Batley, A. Ekstrom, J.J. Fardy, Y.J. Farrar, J. Inorg. Nucl. Chem. 37 (1975) 1961–1966.
[229] K.A. Kraus, F. Nelson, G.L. Johnson, J. Am. Chem. Soc. 71 (1949) 2510–2517.
[230] K.A. Kraus, F. Nelson, J. Am. Chem. Soc. 71 (1949) 2517–2522.
[231] F. Nelson, K.A. Kraus, J. Am. Chem. Soc. 73 (1951) 2157–2161.
[232] T.W. Newton, F.B. Baker, Inorg. Chem. 4 (1965) 1166–1170.

[233] H. Imai, Bull. Chem. Soc. Jpn. 30 (1957) 873–881.
[234] D.M.H. Kern, E.F. Orlemann, J. Am. Chem. Soc. 71 (1949) 2102–2106.
[235] B. McDuffie, C.N. Reilley, Anal. Chem. 38 (1966) 1881–1887.
[236] K.R. Howes, A. Bakac, J.H. Espenson, Inorg. Chem. 27 (1988) 791–794.
[237] T. Privalov, P. Macak, B. Schimmelpfennig, E. Fromager, I. Grenthe, U. Wahlgren, J. Am. Chem. Soc. 126 (2004) 9801–9808.
[238] P. Macak, E. Fromager, T. Privalov, B. Schimmelpfennig, I. Grenthe, U. Wahlgren, J. Phys. Chem. A 109 (2005) 4950–4956.
[239] F. Réal, V. Vallet, U. Wahlgren, I. Grenthe, J. Am. Chem. Soc. 130 (2008) 11742–11751.
[240] S.A. Gaziev, N.A. Gorshkov, L.G. Mashirov, D.N. Suglobov, Radiokhimiya 28 (1987) 755–763.
[241] A.L. Buchachenko, I.V. Khudyakov, Russ. Chem. Rev. 60 (1991) 1105–1127.
[242] A.B. Yusov, V.P. Shilov, Russ. Chem. Bull. 49 (2000) 1925–1953.
[243] K. Okuyama, Y. Ishikawa, Y. Kato, H. Fukutomi, Bull. Res. Lab. Nucl. React. (Tokyo Inst. Technol.) 3 (1978) 39–50.
[244] W.-S. Jung, Y. Ikeda, H. Tomiyasu, H. Fukutomi, Bull. Chem. Soc. Jpn. 57 (1984) 2317–2318.
[245] Y. Kato, H. Fukutomi, J. Inorg. Nucl. Chem. 38 (1976) 1323–1328.
[246] L.P. Spencer, P. Yang, B.L. Scott, E.R. Batista, J.M. Boncella, J. Am. Chem. Soc. 130 (2008) 2930–2931.
[247] T.W. Hayton, J.M. Boncella, P.D. Palmer, B.L. Scott, E.R. Batista, P.J. Hay, Science 310 (2005) 1941–1943.
[248] T. Hayton, G. Wu, J. Am. Chem. Soc. 130 (2008) 2005–2014.